Ocean acidification induces distinct transcriptomic responses across life history stages of the sea urchin *Heliocidaris erythrogramma*

Running head: Expression response to OA across life cycle

Hannah R. Devens[1*], Phillip L. Davidson[1*], Dione J. Deaker[2], Kathryn E. Smith[3], Gregory A. Wray[1,4**], and Maria Byrne[2,5**]

1. Department of Biology, Duke University, Durham, NC 27708, USA.
2. School of Life and Environmental Science, The University of Sydney, NSW 2006, Australia
3. The Laboratory, The Marine Biological Association, Citadel Hill, Plymouth, PL1 2PB, UK
4. Center for Genomic and Computational Biology, Duke University, Durham, NC 27708, USA.

*Contributed equally

**Corresponding authors: gwray@duke.edu; maria.byrne@sydney.edu.au

ABSTRACT

Ocean acidification (OA) from seawater uptake of rising carbon dioxide emissions impairs development in marine invertebrates, particularly in calcifying species. Plasticity in gene expression is thought to mediate many of these physiological effects, but how these responses change across life history stages remains unclear. The abbreviated lecithotrophic development of the sea urchin *Heliocidaris erythrogramma* provides a valuable opportunity to analyze gene expression responses across a wide range of life history stages, including the benthic, post-metamorphic juvenile. We measured the transcriptional response to OA in *H. erythrogramma* at three stages of the life cycle (embryo, larva, and juvenile) in a controlled breeding design. The results reveal a broad range of strikingly stage-specific impacts of OA on transcription, including changes in the number and identity of affected genes; the magnitude, sign, and variance of their expression response; and the developmental trajectory of expression. The impact of OA on transcription was notably modest in relation to gene expression changes during unperturbed development and much smaller than genetic contributions from parentage. The latter result suggests that natural populations may provide an extensive genetic reservoir of resilience to OA. Taken together, these results highlight the complexity of the molecular response to OA, its substantial life history stage specificity, and the importance of contextualizing the transcriptional response to pH stress in light of normal development and standing genetic variation to better understand the capacity for marine invertebrates to adapt to OA.

Keywords: climate change, echinoid, direct development, ocean acidification, RNA-seq, transcriptomics

-

INTRODUCTION

Increased ocean uptake of carbon dioxide (CO_2) due to rising anthropogenic emissions is causing rapid alterations to the biological, chemical, and physical composition of the marine environment (Gattuso et al., 2015; IPCC, 2014). These changes have resulted in a multidimensional set of stressors for marine life as the ocean becomes more hypercapnic (increasing pCO_2), more acidic, and less saturated in calcium carbonate minerals (Albright et al., 2016; Gattuso et al., 2015; IPCC, 2014). Calcifying marine invertebrates such as corals, mollusks, and echinoderms are particularly vulnerable to the reduced availability of carbonate ions (Byrne & Hernandez, 2020; Kroeker et al., 2013; A. M. Smith, Clark, Lamare, Winter, & Byrne, 2016). Several studies have shown the negative effect of decreasing carbonate mineral saturation on skeletogenesis in these animals (Byrne & Fitzer, 2019; Byrne, Lamare, Winter, Dworjanyn, & Uthicke, 2013; Collard, Catarino, Bonnet, Flammang, & Dubois, 2013; Stumpp, Wren, Melzner, Thorndyke, & Dupont, 2011). Hypercapnic seawater conditions and reduced pH can also disrupt metabolism, resulting in the prioritization of energy reserves toward the maintenance of essential physiological processes (e.g., acid-base homeostasis) rather than growth and calcification (Byrne et al., 2013; Carey, Harianto, & Byrne, 2016; Collard et al., 2013; Liu et al., 2020; Stumpp et al., 2011; Todgham & Hofmann, 2009).

The impact of OA on the reproduction, development, and physiology of marine invertebrates differs between species (Kroeker et al., 2013; Przeslawski, Byrne, & Mellin, 2015), and gene expression studies indicate that the affected physiological and molecular pathways also differ (Strader, Wong, & Hofmann, 2020). The ability to measure the expression of all genes simultaneously through transcriptomic analyses provides a powerful approach to understanding organism responses and differences among taxa, as this approach affords a comprehensive and

unbiased view of stress response at the molecular level. Several studies have used this approach to examine the effects of OA in diverse marine invertebrates, with a major focus on calcifiers, as they are the most vulnerable (Davies, Marchetti, Ries, & Castillo, 2016; De Wit, Durland, Ventura, & Langdon, 2018; Evans, Chan, Menge, & Hofmann, 2013; Griffiths, Pan, & Kelly, 2019; Maas, Lawson, Bergan, & Tarrant, 2018; Pan, Applebaum, & Manahan, 2015; Strader et al., 2020). To date, no study has examined the transcriptomic response to OA spanning the planktonic to benthic transition in any marine invertebrate (for a recent review, see Strader et al., 2020). To address this gap in knowledge, we carried out transcriptomic analyses of the response to OA at three life history stages (embryos, larvae, and metamorphosing juveniles) under control and OA conditions in the sea urchin *Heliocidaris erythrogramma*.

H. erythrogramma is abundant in shallow benthic habitats around temperate Australia where, like many sea urchin species, it is ecologically important in structuring subtidal habitats as a major grazer of macroalgae (Keesing, 2020). Prior studies of the impact of OA on survivorship and morphogenesis of *H. erythrogramma* demonstrate that fertilization, embryos, and early larvae are robust to projected OA conditions (pH 7.6-7.8) (Byrne et al., 2010; Hardy & Byrne, 2014), while later metamorphic stages are more sensitive to these pH levels (Byrne et al., 2011). *H. erythrogramma* develops rapidly through a lecithotrophic (nonfeeding) larva (Williams & Anderson, 1975), providing an opportunity to examine the effects of OA on gene expression across the life cycle from embryo to early juvenile for the first time in a marine invertebrate.

Because the evolution of lecithotrophy in *H. erythrogramma* involved substantial changes in maternal provisioning, developmental physiology, and larval anatomy (Byrne & Sewell, 2019; Davidson et al., 2019; Henry, Wray, & Raff, 1990; M. S. Smith, Collins, & Raff, 2009; Williams & Anderson, 1975), the response of development in this species to OA would be expected to

differ with respect to the larval stage (i.e. feeding vs non-feeding sea urchin larvae). In particular, the larval skeleton is reduced to vestigial spicules in *H. erythrogramma* compared with the well-developed skeleton of echinoplutei (Emlet, 1995; Williams & Anderson, 1975) and so may be less susceptible to the effects of OA during pre-metamorphic stages of the life cycle. For the Echinodermata, species with nonfeeding and noncalcifying larvae have exhibited differential survival through past extinction events, including those linked to altered climate (Uthicke, Schaffelke, & Byrne, 2009). Furthermore, genomic resources are available for *H. erythrogramma*, including developmental transcriptomes (Israel et al., 2016; Wygoda, Yang, Byrne, & Wray, 2014), as well as metabolic and proteomic mass spectrometry datasets (Davidson et al., 2019), making this a particularly valuable species for studying transcriptomic responses to OA.

Besides carrying out conventional analyses to identify differences in transcript abundance, we examined two other informative features of the gene expression response to OA. First, we measured variance in gene expression, both for individual genes based on variance partitioning and for the transcriptome as a whole based on the variance-to-mean ratio (VMR). Because increased variance can reflect misregulation (Felix & Barkoulas, 2015; Lopez-Maury, Marguerat, & Bahler, 2008), these measures provide a way to gauge whether OA disrupts the regulation of gene expression as distinct from the reaction norm. Second, we measured changes in the shape of gene expression profiles across developmental stages, based on soft clustering (Kumar & Futschik, 2007) and changes in cluster membership (Israel et al., 2016). Such "cluster jumps" provide an objective method for identifying large changes in the temporal trajectory of gene expression independent of expression level (e.g., progressive increase *vs* central peak). Finally, we took advantage of the controlled breeding design to measure genetic contributions to the transcriptomic

response to OA using male parent as a factor in a mixed linear model (Runcie et al., 2016). Taken together, the results of these analyses illustrate the value of examining diverse facets of the molecular response to a stressor, sampling multiple life history stages, and measuring the relative magnitude of genetic and environmental influences on gene expression.

MATERIALS AND METHODS

Experimental design and set up

Heliocidaris erythrogramma adults were collected near Sydney, Australia and maintained in flow-through filtered natural seawater (FSW, 20 μm) at the Sydney Institute of Marine Sciences. A controlled breeding design consisting of three crosses was used, with each cross derived from eggs pooled from the same five females and sperm from a different male. Pooling eggs from five females provided sufficient biological material for sampling multiple time points, while fertilizing with sperm from different males provided biological replication as well as the ability to estimate male genetic contributions to variation in gene expression among samples (Runcie et al., 2016). An asymmetric breeding design was used because female genetic contributions are difficult to measure during development due to differences in egg quality that often overwhelm genetic differences, while male contributions are considered nearly equivalent to genetic contributions as sperm bring few nutrients and mRNAs to the zygote (Lynch & Walsh, 1998).

Spawning was induced by injecting 0.5 ml of 0.5 M KCl into the coelom. Eggs and sperm were microscopically checked for quality and motility and the sperm of three males was stored dry until use. Equal portions of eggs from five females were combined in a 5 L beaker of FSW and aliquots were counted to determine egg concentration. Eggs were then divided equally across three 5 L beakers of FSW at experimental pH_T levels (8.0 and 7.6; see below for details). To generate

three biological replicates, eggs were fertilized in each beaker with sperm from a different male at a concentration of 10^4 sperm/mL (determined by hemocytometer counts), resulting in three distinct crosses for each pH condition with fertilization rate > 90%. Embryos were reared at a concentration of 1/mL in 100 mL plastic containers in a flow-through seawater system (1.0 µm FSW) with water at experimental pH_T levels and temperature at 20°C.

The two pH_T conditions in our experiment, pH_T 8.0 and pH_T 7.6, represent current and projected future ocean pH_T (2100) (IPCC, 2014). The shallow subtidal environments in eastern Australian coastal areas, where *H. erythrogramma* are typically found, fluctuate between pH_T 7.87 - 8.30 (Wolfe, Nguyen, Davey, & Byrne, 2020); thus, a pH_T of 7.6 is likely to be outside their natural pH range. The pH_T of seawater was maintained using a mixed CO_2 system, in which a thermally compensated, low-flow controller valve (Parker Hannifin, OH, USA) and a proportional-integral-derivative controller, updated every 10 s, were used to inject food-grade CO_2 into ambient air that had been scrubbed of CO_2. CO_2 was vigorously and continuously bubbled into the header tank, using ceramic diffusers to supply pH_T 7.6 water. Ambient seawater in the controls was not manipulated. A thermocouple-solenoid feedback system that automatically mixed warm and cold water in a mixing chamber was used to supply water at stable temperature (20°C) at the desired pH_T. Seawater pH was measured spectrophotometrically on the total scale (pH_T) with a custom-built sampling system connected to an Ocean Optics USB4000+fiber optic spectrometer using m-Cresol dye indicator (Acros Argonics lot #A0321770) and pH_T was calculated according to Liu, Patsavas, and Byrne (2011).

Measurements were calibrated to certified reference material (CRM) for CO_2 in seawater (Batch 139 (A. G. Dickson, Sabine, C.L., & Christian, J.R., 2007)). In parallel with pH monitoring (see below), samples (330 mL) of source water were collected daily over the five

days of rearing to determine total alkalinity (TA) by potentiometric titration (Titrando, Metrohm) (see Supp. Table 1) calibrated using seawater CRMs (Batch 139 (A. G. Dickson, Sabine, C.L., & Christian, J.R., 2007); carbonate system parameters, pCO_2, calcite and aragonite saturation states were calculated using CO2SYS (Pierrot, 2006) (Supp. Table 1). Dissociation constants for these calculations were calculated following Mehrbach, Culberson, Hawley, and Pytkowicx (1973) as refit by A. G. Dickson and Millero (1987) for K1/K2 and Andrew G. Dickson (1990) for $KHSO_4$, and Uppström (1974) for total boron. Temperature and pH were monitored daily in all treatments in numerous randomly selected rearing containers at the level of the developing H. erythrogramma using a WTW multimeter (WissenschaftilichTechnischeWerkstatten GmbG P4) and SenTix_ 41 pH electrode; precision_0.01 pH units) to ensure conditions remained on target. The probes were calibrated using NIST high precision buffers pH 4.0, 7.0 and 10.0 (ProSciTech, Australia) with pH on the total scale determined through calibration with TRIS sea water buffer using the millivolt scale (A. G. Dickson, Sabine, C.L., & Christian, J.R., 2007). The pH_T levels were the same across all rearing containers per treatment and so the daily pH_T measure was used to determine the carbonate chemistry parameters (Supp. Table 1). FSW was supplied at the appropriate pH_T by a dripper tap system to individual containers. FSW was supplied at the appropriate pH_T by a dripper tap system to individual containers fitted with 150 µm mesh-covered windows that maintained 40-50 mL of water in the containers at all times, with a flow rate of ~ 3-4 mL/min.

Following fertilization, each of the three crosses was divided into two equal portions and reared at the different pH_T levels, using 6-8 separate vessels for each cross X treatment in order to achieve low culture densities. Samples were collected at three time points: embryo (gastrula stage, 26 hours post fertilization (hpf)), early larva (48 hpf), and newly settled juvenile (108 hpf) (see Fig.

1). Metamorphosis is not synchronous in *H. erythrogramma* cultures, so settled, post-metamorphic individuals were hand-picked to sample the juvenile stage to ensure that they were at a similar stage of development. Previous studies have shown that early embryos of *H. erythrogramma* are resilient to OA with increased sensitivity to the juvenile stage and differential survival of resilient progeny (Byrne et al., 2009; Byrne et al., 2011; Hardy & Byrne, 2014). In total, 18 samples were collected for RNA-sequencing (3 developmental stages x 2 pH conditions x 3 biological replicates). It was not possible to measure mortality, as dead embryos and larvae disintegrate quickly and were washed out of the flow-through culture system used here. We monitored the developing stages closely and did not note developmental delay in response to OA.

RNA extraction and sequencing

Approximately 50 individuals were collected for each RNA sample and placed in TRIzol (Invitrogen) for RNA extraction according to the manufacturer's instructions. Samples were diluted in 40mL RNase-free water and stored at -80° C. RNA concentration was measured by Qubit (Thermo Fisher Scientific) and RNA quality was determined with a Fragment Analyzer and PROSize 2.0 (Agilent). In total, 17 samples were sequenced. One sample (8_1M1L: pH_T 8.0, Male 1, Larva) was not processed due to poor RNA quality. Library synthesis and sequencing of the RNA samples were carried out at the Sequencing and Genomic Technology shared resource at the Duke University Center for Genomic and Computational Biology. Sequencing libraries were synthesized with KAPA Stranded mRNA-Seq kits (Roche). Paired-end sequencing greatly aids in the construction of a de-novo transcriptome, but is cost-prohibitive to conduct on all samples; therefore, samples were randomly subjected to either 150bp paired-end or 50bp single-end sequencing (see Supp. Table 2 for sequencing scheme) on an Illumina HiSeq 4000 platform to maximize transcriptome quality while optimizing cost.

Read quality control

Read quality and summary statistics were generated with FastQC (Andrews, 2010) and read trimming and adapter removal performed using Trimmomatic v. 0.38 (Bolger, Lohse, & Usadel, 2014) with the following parameters: LEADING:10, TRAILING:10, SLIDINGWINDOW:4:15, MINLEN:30. Putative ribosomal RNA (rRNA) reads were identified and removed from paired-end reads (because these reads ultimately were used for *de-novo* transcriptome assembly) by aligning reads with Bowtie2 v. 2.2.4 (Langmead & Salzberg, 2012) to reference metazoan rRNA sequences retrieved from the Agalma transcriptome assembly pipeline (Dunn, Howison, & Zapata, 2013). In addition to the RNA-seq reads generated in this study, 50bp paired-end reads from Wygoda et al., 2014 and Israel et al., 2016, which encompass egg through 10-day post-metamorphosis in *H. erythrogramma,* were incorporated into our *de-novo* transcriptome assembly workflow to generate a more comprehensive developmental transcriptomic reference. Raw reads from these two studies were subjected to the same quality control measures as the sequencing reads generated in this study prior to assembly.

Transcriptome assembly and transcript abundance estimation

Trimmed forward and reverse paired-end reads were concatenated along with paired-end reads from two previous studies (Israel et al., 2016; Wygoda et al., 2014) into "master" forward- and reverse-oriented FASTQ files. To reduce the large computational demands of *de novo* transcriptome assembly from ~1.3 billion reads, forward and reverse reads were subjected to *in silico* normalization within Trinity v. 2.0.6 (Grabherr et al., 2011) (parameters: k-mer length = 25, maximum read coverage = 50). These normalized reads were used as input for *de novo* transcriptome assembly in Trinity v. 2.0.6 under default parameters. Following assembly, contigs from putative non-metazoan contaminant reads were identified and removed from the

transcriptome with *alien_index* (Ryan, 2015). Highly similar contigs were clustered with the *cd-hit-est* program of CD-HIT (Li & Godzik, 2006) to remove highly redundant reference sequences within the transcriptome (parameters: c = 0.90, n = 9, l = 10). Transcriptome summary statistics were generated by Transrate (Smith-Unna, Boursnell, Patro, Hibberd, & Kelly, 2016) and are available in Supp. Table 3. Lastly, contigs were annotated with protein models from the well-studied sea urchin species *Strongylocentrotus purpuratus* (Sea Urchin Genome Sequencing et al., 2006) using BLAST-X (Altschul, Gish, Miller, Myers, & Lipman, 1990) at an e-value threshold of 1e-10. To minimize quantification bias between single-end and paired-end samples, only forward reads from paired-end samples that were trimmed to 50 bp were used for mRNA abundance estimation within these samples. Trimmed reads were aligned to the transcriptome and transcript abundance estimates were made with Salmon (Patro, Duggal, Love, Irizarry, & Kingsford, 2017). Transcript abundance estimates were imported into R via the *tximport* library (Soneson, Love, & Robinson, 2015) for statistical analysis.

Count filtering and differential expression analyses

Isoform-level contigs at the gene level were combined via *tximport* and counts from contigs mapping to the same *S. purpuratus* gene model were summed together. The resulting dataset contained 19,728 genes. Genes with fewer than 2 counts-per-million (CPM) were removed from this list, leaving 15,322 genes for use in downstream analyses; these counts are available in Supp. Data 1. Principal component analysis (PCA) was conducted using the *prcomp* function within R on transposed *rlog*-transformed counts plus one pseudocount (rlog[count + 1]) to identify the contribution of each factor in the experiment to variation among samples. Differential expression analyses were performed using DESeq2 v1.20.0 (Love, Huber, & Anders, 2014). Specifically, a DESeqDataSet was constructed on the 15,322 genes to test for differential transcript abundance

between pH conditions (model: ~group where "group" is pH and Stage combinations; i.e. CL = control at larval stage). Individual differential expression results at each stage were then extracted using the "contrast" argument of the *results* function in DESeq2. The use of groups and contrasts allowed us to ensure that the loss of one sample (at the larval stage at control pH) did not bias our stage-to-stage results. In testing the effects of the loss of one sample, we found that artificially removing another sample from the same male at a different stage *did* affect the number of DE genes at each stage, but that this effect was proportional and did not change our overall conclusions about the relative number of DE genes among stages.

Because we anticipated that the effect of pH would be subtle relative to other factors of the experiment based on our earlier study (Runcie et al., 2016), genes with FDR (false discovery rate)-corrected p-values ≤ 0.10 were considered significantly differentially expressed between sample groups (Supp. Data 2). Current RNA-seq best practices do not include recommendations for fold change (FC) thresholds for differential expression so long as there is an appropriate number of biological replicates (Conesa et al., 2016; Zhang et al., 2014). However, in order to provide a direct comparison with previous OA studies, a log2(FC) threshold > = 1.5 in conjunction with our significance cutoff was separately applied and examined independently in downstream analyses. Considering differentially expressed genes both with and without FC thresholding guards against the tendency of biological interpretations to change based on the threshold selected (Dalman, Deeter, Nimishakavi, & Duan, 2012; Schurch et al., 2016). Lists of differentially expressed genes at each stage are presented in Supp. Data 2 and overlaps between stages plotted as area-proportional diagrams using eulerAPE 3.0 (Micallef & Rodgers, 2014). Differentially-expressed genes were compared with 890 genes found to be OA-responsive in previous studies (Evans, Pespeni,

Hofmann, Palumbi, & Sanford, 2017; Evans & Watson-Wynn, 2014) to determine how many of the genes found in our study had not previously been reported to be OA-sensitive.

Variance partitioning and VMR analyses

Variance partitioning of transcript abundances was carried out using the R package "variancePartition" (v1.12.1) (Hoffman & Schadt, 2016), which fits a linear mixed model to each gene in the dataset and estimates the fraction of total variance attributable to each factor in the experimental design. All variables (paternal effect; pH; the interaction of pH and paternal effects (pH:Male)) were modeled as random effects in accordance with the recommendations of the variancePartition manual, which suggests modeling categorical variables as random effects. Genes for which at least 10% of expression variance could be attributed to pH were considered to have significant variance changes due to pH (59 genes) (Supp. Data 3).

Variance-to-mean ratio analysis was carried out by first calculating the variance of each gene at a given sample group (stage, pH), and then dividing this value by the mean expression of that gene for that sample group. Density plots were created (using the *geom*_density function within the R package ggplot2) for the VMR of all genes at each stage and pH condition. Statistically significant differences between VMR density distributions were determined using the built-in R function *ks.test* to perform Kolmogorov-Smirnov (K-S) tests for equality. To determine whether the average VMR at each stage was significantly different between pH treatments, a two-sided paired t-test was used.

Soft clustering time course analyses

For comparative developmental time course analysis, raw counts of the 15,322 genes included in the differential expression analyses (see above) were normalized with the DESeq2-regularized log (*rlog)* transformation (Supp. Data 4). Soft clustering of temporal gene expression

profiles was carried out with the R package *Mfuzz* v. 2.40.0 (Kumar & Futschik, 2007). Prior to clustering, mean expression values were calculated for each gene at each developmental stage and genes with the lowest 5% standard deviation *across* development were filtered out so as to remove genes whose expression changed minimally over time. This procedure yielded 14,595 genes to be included in expression cluster profiling. Initially, samples from both pH treatment groups were included to create a reference set of cluster profiles. The fuzzification coefficient (m) was determined to be 3.601 via the *mestimate* function of the *Mfuzz* package. The *Dmin* function, which calculates the minimum centroid distance between varying numbers of clusters, was used to estimate the optimal number of clusters as 5 (Supp. Fig. 1).

Because the fuzzy clustering method employed here is not a deterministic process, the clustering procedure was repeated 1,000 times and the cluster iteration with the lowest objective function value was selected to maximize accuracy and representation of gene expression profiles among the five clusters. Next, pH_T 8.0 and pH_T 7.6 samples were separately mapped to this reference set of clusters to calculate membership values of every gene to one of five clusters. To increase confidence of cluster assignments, genes in both pH_T 8.0 and pH_T 7.6 samples were required to have a minimum membership score of at least 0.3 to be assigned a cluster. Genes whose cluster membership differed between control and acidic treatments (termed "cluster jumpers"; Israel et al., 2016) were identified, resulting in a set of 2,831 genes whose temporal expression profile changed between pH conditions (Supp. Data 5: cluster memberships; Supp. Data 6: plots of gene expression profiles).

Enrichment analyses of biological function

Gene ontology (GO) enrichment analyses were performed on gene sets of interest via the *runGSAhyper* function of the R package "piano" v. 1.22.0 (Varemo, Nielsen, & Nookaew, 2013),

including Benjamini-Hochberg FDR correction for multiple comparisons (Benjamini, Drai, Elmer, Kafkafi, & Golani, 2001). Along with GO terms associated with *S. purpuratus* gene models (retrieved from Echinobase: www.echinobase.org/Echinobase), we included additional sea urchin specific gene sets in the enrichment analyses, including primary mesenchyme effector genes (Rafiq, Shashikant, McManus, & Ettensohn, 2014) and genes categorized as putatively involved in "biomineralization" (also retrieved from Echinobase). The latter two categories were included to capture gene expression responses associated with the skeleton, which is an autapomorphy of the phylum and thus not represented in GO and other general functional ontologies. See Supp. Data 7 for enrichment analysis results. Because GO annotations do not always correlate with biological function in sea urchins (Evans et al. 2017), categorical enrichment tests were also performed using functional categories from EchinoBase. These were run as 2-sample tests for equality of proportions with continuity correction against the list of genes expressed in our entire dataset.

Density plots of mean gene expression by parentage

At a given stage, the mean normalized count was calculated for each gene across the three genetic crosses. Then, the percent difference from this mean for each genotype was calculated as a relative change, according to the equation

$$(Sire_n - Sire_{\bar{x}}) / Sire_{\bar{x}}$$

where $Sire_n$ is the normalized count from one of the three genotypes and $Sire_{\bar{x}}$ is mean the normalized count across the three genotypes. The percent differences for all genes and genotypes were then plotted in a density distribution for each stage and pH condition. To determine if the density plots of each genotype within a stage were different from one another, we used two-way K-S tests of equality (as described above) for each possible pair of male genotypes.

-

RESULTS

Scope and magnitude of transcriptional responses to OA

Reduced pH induced changes in the expression of 50, 61, and 797 genes in embryos, larvae, and juveniles, respectively (Fig. 2; Supp. Data 2) using the standard dispersion-based approach to identifying differential expression in RNA-seq data (Anders et al., 2013; Conesa et al., 2016; Love, Anders, Kim, & Huber, 2015; Love et al., 2014; Mark et al., 2019; Walker et al., 2019; Zhang et al., 2014). Only eight of these genes (< 1%) were differentially expressed at more than one developmental stage, and just one was differentially expressed at all three stages (Fig. 3A). Interestingly, the gene that was differentially expressed at all three stages, *Taf5L* (SPU_020698), encodes a transcription co-factor. Of the eight genes that were differentially expressed at more than one stage, the sign of the response differed (up- and down-regulated) among stages in three cases (Supp. Table 6). These results indicate that OA induces changes in transcription among largely distinct sets of genes at different stages of the life cycle.

Most changes in transcript abundance were modest, and rarely exceeded 1.5-fold (which we consider to be a "large" fold change in this study). Each time point showed a markedly different response to OA in terms of effect size: most of the large fold-changes in gene expression were found in embryos, while larvae had only one gene with a large fold-change, and juveniles showed a marked bias towards down-regulation among genes with the largest (for this stage, but not overall) fold-changes (Fig. 2, red dots). These results indicate that OA induces quantitatively distinct responses in gene expression at different stages of the life cycle. Of note, the largest transcriptional responses to reduced pH are orders of magnitude smaller than the largest changes in gene expression that take place during unperturbed development: in control cultures, the number of genes showing ≥ 100-fold change between stages was 50 (embryo to larva), 115 (larva to

juvenile), and 383 (embryo to juvenile) using an adjusted p-value of ≤ 10%. In contrast, no gene showed such a large expression change in response to pH treatment at any of the three stages examined.

Principal component analysis of normalized gene expression counts reinforced these findings, indicating that most of the variance among the transcriptomes of *H. erythrogramma* was attributable to developmental stage. Principal components 1 and 2 both discriminated samples by stage, and together accounted for more than 91% of expression variance (Fig. 4A; Supp. Table 4). A linear mixed model also found that developmental stage accounts for the majority of differences in gene expression: an average of 48.9% of variation in expression per gene was explained by stage, while male parent (a proxy for genetic effects; see Lynch and Walsh (1998)) and pH treatment explained just 6.5% and 0.2% of variation, respectively (Supp. Data 3). These results indicate that the response to OA involves far fewer genes, and much smaller changes in transcript abundance, than the changes that take place during the course of normal development.

Effects of OA on stage-specific transcript abundance

In embryos, 50 genes were differentially expressed in response to OA in *H. erythrogramma* (Fig. 2A; Supp. Data 2). According to Echinobase functional categorizations, these included three genes with biomineralization function (*Msp130* SPU_002088, *Msp120or4* SPU_014496, *Msp130or5* SPU_015763), two calcium toolkit genes (*Hsp701B* SPU_005808, *Hsp701C* SPU_009477), five encoding chaperone proteins (*DnaJB1/HSP40* SPU_002148, SPU_005807, SPU_008985, SPU_009479, *Sap30L* SPU_027083), and four genes putatively involved in the defensome (*HSP70_L2* SPU_009476, *HSP70_L* SPU_009478, *Cyp2L26* SPU_013039, *HSP701D* SPU_016500). Among the most differentially expressed genes at pH_T 7.6 (log_2 fold change > 1.5) were five genes coding for proteins in the heat shock protein family, including two encoding

paralogues of *HSP70* (SPU_009476, SPU_009478). These *HSP70* genes were down-regulated at pH_T 7.6, similar to the response of *HSP70* reported for the planktotrophic larvae of *S. purpuratus* (Todgham & Hofmann, 2009).

In larvae, 61 genes showed differential expression in response to OA (Fig. 2B; Supp. Data 2). Only three of these overlapped with differentially expressed genes in embryos: *Msp130* (SPU_002088) was upregulated at both stages, while *Wipf1L* (SPU_013094) and *Taf5L* (SPU_020698) showed discordant responses. Nonetheless, several genes involved in similar biological processes were differentially expressed under OA conditions at both embryonic and larval stages (Supp. Data 2). Of particular interest are genes in the *Msp130* family, which encode proteins essential for biomineralization (Anstrom, Chin, Leaf, Parks, & Raff, 1987; Karakostis et al., 2016; Killian & Wilt, 2017; Leaf et al., 1987). *Msp130* (SPU_002088) expression was up-regulated in embryos and larvae of *H. erythrogramma* in response to OA, while four paralogues, *Msp130_1* (SPU_013821), *Msp130r3* (SPU_013823), *Msp130r4* (SPU_014496), and *Msp130r5* (SPU_015763), were also up-regulated in either or both embryos and larvae. Several prior studies have reported changes in *Msp130* expression in response to OA in sea urchin larvae, in one case increasing (Martin et al., 2011) and in others decreasing (Di Giglio et al., 2020; Kurihara, Takano, Kurokawa, & Akasaka, 2012; Stumpp et al., 2011).

In metamorphosing juveniles, the transcriptomic response to OA was notably distinct from the two earlier stages: more than 10 times as many genes (797) were differentially expressed, and there was a strong bias towards down-regulation (Fig. 2C; Supp. Data 2). Genes with altered expression included several involved in transcriptional regulation, the calcium toolkit, biomineralization, and immune response (Echinobase functional categorization; Supp. Data 2), with statistically significant enrichments in the “cytoskeleton” and “calcium toolkit” functional

categories relative to the transcriptome as a whole (p < 3.5e-12 and p < 3.98e-2, respectively). Many pH-responsive genes in *H. erythrogramma* juveniles were similar to those reported for sea urchins with planktotrophic larvae, with 38 differentially expressed genes in *H. erythrogramma* juveniles previously reported to be responsive to OA stress during pre-metamorphic development in planktotrophic species (Evans & Watson-Wynn, 2014) (Supp. Table 5). (Direct comparison to OA transcriptomic response in juveniles of a planktotrophic sea urchin is not possible as none have been published.) The previously-reported genes that were also differentially regulated here include two encoding beta-tubulin (*Btub3* SPU_000062 and *Btub2_1* SPU_001045) that showed decreased expression at low pH in *H. erythrogramma* (this study) and *S. purpuratus* (Padilla-Gamino, Kelly, Evans, & Hofmann, 2013), as well as three metabolic genes (*Ak9L2* SPU_020625, *Ak7* SPU_010764, *Ckb* SPU_015323) and two calcium toolkit genes (*Slc8a1* SPU_006810, *CacTta1Hs* SPU_014334) (Evans & Watson-Wynn, 2014). Although many genes and biological processes previously reported to be OA-sensitive were also differentially expressed in our study (Supp. Table 5), the majority of the individual genes we report as differentially expressed have not been previously reported to be OA-sensitive.

Effects of OA on stage-specific variance in gene expression

Increased variance in gene expression in response to a stressor may point to compromised transcriptional regulation (Felix & Barkoulas, 2015; Lopez-Maury et al., 2008) and can be measured for the transcriptome as a whole as the variance-to-mean ratio (VMR). We found that the overall VMR among biological replicates was higher at pH_T 7.6 than pH_T 8.0 at embryo and larval stages, but not in juveniles (Fig. 5; Supp. Fig. 3; two-sided paired t-test p-value < 0.05). This increase was most pronounced in larvae (p-value < $1x10^{-6}$, 31.4% overall increase in VMR). An increase in VMR at lower pH was evident across several categories of gene function in larvae

(Supp. Fig. 4), indicating that this effect was not driven by a single biological pathway or process but instead affected genes associated with a broad range of biological functions.

A stressor's impact on variance in expression of individual genes can be captured through the linear mixed model mentioned earlier. This approach revealed that, while average contribution of pH to variance was low relative to other factors, pH explained at least 10% of expression variation for 59 genes (Supp. Data 3). Considering that the average pH contribution to variance for all genes was just 0.2% (see above, *Scope and magnitude of transcriptional responses to OA*), this result suggests that transcriptional regulation of these 59 genes is particularly sensitive to acidification. Of these genes, four are associated with defensome functions (*Cyp4L1* SPU_005931, *Cyp4L_2* SPU_007335, *Hsp701F* SPU_013289, *Osta* SPU_019774), seven with metabolism (*Sds* SPU_013298, *Slc25a36* SPU_017892, *Slsp_5* SPU_018147, *Sgpl1_1* SPU_020002, SPU_023931, *Scly* SPU_024173, *Ctso* SPU_027818) and two with immune function (*Ndufa13* SPU_024115, *Irf* SPU_010404). Of note, many of these genes (32 of 59) for which OA contributed substantially to expression variation were not identified as differentially expressed at any stage (Fig. 3B).

Effects of OA on multistage gene expression trajectories

While measures of differential expression and expression variance at a single stage are useful for identifying stress responses, they provide just one "snapshot" of the molecular response to low pH exposure. Soft clustering (Kumar & Futschik, 2007) provides a tool for determining how temporal patterns, rather than relative levels, of gene expression change under OA relative to control conditions. Using this method, 14,595 genes expressed in both control and OA conditions were assigned to one of five clusters representing temporal expression profiles (Fig. 6; Supp. Data 5). Comparison of the assigned cluster for each gene under control and OA conditions provides an

unsupervised method for distinguishing temporal patterns of gene expression that are unaffected from those that are impacted by exposure to the stressor.

Most genes (80.6%) remained in the same cluster, indicating that their temporal expression profiles were similar under both pH treatments (Fig. 6, boxes on the diagonal). The remaining 2,831 genes were assigned to a different cluster at reduced pH, indicating a change in the shape of their gene expression trajectory during development ("cluster jump"; see Israel et al. 2016). As expected, moderate changes in expression trajectory were the most common; for 240 genes, however, the change was more substantial (Fig. 6; boxes directly adjacent to the diagonal *vs* those further away). Relative to the transcriptome as a whole, cluster-jumping genes were significantly enriched for the zinc finger and DNA functional categories, as well as for GO terms such as RNA-dependent DNA replication, DNA repair, DNA-templated transcription, and ribosome biogenesis (Supp. Data 7). Only 38.0%, 31.1%, and 18.7% of genes identified as differentially expressed between pH conditions at the embryo, larva, and juvenile stages, respectively, were also classified as cluster-jumping genes (Fig. 3B; Supp. Data 8).

Impact of genetic variation on transcription

The linear mixed model mentioned earlier estimated that the impact of variation in male genotype (a proxy for genetic influences) on variation in gene expression throughout the transcriptome was approximately 325 times greater than the impact of reduced pH (Fig. 4B), even though our experimental design is weakly powered to detect parent-of-origin effects. The interaction of male genotype and pH was relatively modest, explaining only 0.3% of gene expression variation throughout the transcriptome as a whole. However, this interaction term explained at least 10% of the variation in expression for 131 individual genes (Supp. Data 3). Of

these genes, 11 encode hydrolases, eight are metabolic genes, eight are associated with immune function, and eight encode transferases.

Plotting the density distribution for the deviation of each genetic cross from the mean expression of each gene provides a way to understand how genotype influences transcriptomic response to OA (see Methods). Applying this approach to our data suggests that the different genotypes have varying sensitivities to low pH (Fig. 7). For example, the distribution of deviations from mean gene expression at embryo for each genotype was approximately the same at control pH but became clearly stratified by genotype at low pH. Specifically, expression in the offspring of male 2 was shifted above the average expression of all three genotypes at lower pH, while expression of the offspring of male 3 tended to be below the average expression of all three genotypes. Expression deviations from the mean in larvae also became more stratified at low pH compared to control pH, with some males also showing wider deviation from the mean than others (i.e., offspring of male 1 tended to show expression above the mean expression of all three genotypes, but also showed more spread in expression compared to the other two genotypes at low pH). Loss of the culture from Male 1 at control pH makes it difficult to compare expression between pH levels rigorously; however, the pattern of increased stratification by genotype at low pH was maintained even when we removed the Male 1 culture at low pH from our analyses (data not shown). Curiously, at the juvenile stage there was *more* stratification in expression between genotypes at the control pH than at low pH (i.e., the opposite of the result from the early embryonic stages). Thus, these results indicate that both genotype and genotype-by-environment interactions influence transcription broadly under OA conditions, but this pattern may be restricted to early embryos.

-

DISCUSSION

OA elicits a complex transcriptional response in H. erythrogramma

Several previous studies have examined the gene expression response to OA in sea urchins with planktotrophic larval development (Evans & Watson-Wynn, 2014; Strader et al., 2020) and these differ in the life history stages and methodologies used (Table 1), making comparison of transcriptomic results among studies challenging. Nonetheless, similarities as well as striking differences are evident in our findings with *H. erythrogramma*. Some genes whose expression change in development of sea urchins with feeding larvae under reduced pH conditions were also affected in *H. erythrogramma*, including *HSP70* and *Msp130* (which encode a chaperone and a biomineralization protein, respectively). Biological process categories enriched in differentially expressed genes in *H. erythrogramma* also partially overlapped findings from prior studies, including stress response, calcium toolkit, and biomineralization (Supp. Table 5). These results point to the sensitivity to OA of key genes and cellular processes in sea urchin development. Despite these similarities, most individual genes and a few biological process categories differentially expressed in response to OA in *H. erythrogramma* have not been previously reported. These unique features of the response to reduced pH in *H. erythrogramma* may reflect the range of life history stages sampled here. This is particularly true for the metamorphosing juvenile stage, which has not previously been examined in any sea urchin and which showed by far the greatest number of OA responsive genes (Fig. 3A). Additional differences may reflect the highly derived physiology and developmental mechanisms associated with the lecithotrophic life history of this species (Byrne & Sewell, 2019; Davidson et al., 2019; Henry & Raff, 1990; Wray & Raff, 1990). Differentially expressed genes related to lipid metabolism (*Sgpl1_1,* SPU_020002) and

mitochondrial function (*Slc25a36,* SPU_017892) are especially interesting in light of the lipid-rich eggs of *H. erythrogramma* and are prime candidates for future functional analysis.

Gene expression responses to stressors can manifest in ways other than changes in transcript abundance. Increased variance in gene expression is an informative indicator of stress, and indeed may be a more direct indicator of dysregulation than differential expression (Felix & Barkoulas, 2015; Lopez-Maury et al., 2008). The VMR is a useful measure of variance that can be applied to the transcriptome as a whole. The VMR in transcript abundance increased under OA conditions in embryos and even more so in larvae of *H. erythrogramma*.A general increase in variability of gene expression at low pH could result from compromised mechanisms of transcriptional regulation specifically or homeostatic mechanisms more generally; alternatively, it may reflect a genotype-by-environment interaction, as has been shown in other invertebrates (Chen, Nolte, & Schlotterer, 2015; Webster, Jordan, Hibshman, Chitrakar, & Baugh, 2018). Genes with elevated variance can therefore shed new light on the pH stress response by revealing additional molecular processes that may be affected but did not result in differential expression (Figs. 3B and 7).

A third informative manifestation of the gene expression response to stress is a change in the shape of a developmental trajectory. We used soft clustering to assign each gene to one of five temporal expression profiles that are independent of magnitude, then identified genes whose expression "jumped" to a different cluster under conditions of low pH. Because the expression trajectory of most genes fits into just a few clusters, cluster reassignment reflects a large change in the overall shape of the expression profile across development. Genes that cluster-jumped were enriched in several biological processes, including DNA replication, transcription, and translation. Of note, many genes whose expression profile changed in response to OA were not identified as differentially expressed at any single stage (Fig. 3B). This result illustrates how examining

developmental trajectories can enrich understanding of the biological processes that may be impacted by a stressor.

Both variance and clustering analyses of our results demonstrate that differential expression analyses can miss informative aspects of the molecular response to OA (Figs. 3B and 7). This is likely because each metric (mean, variance, and trajectory) captures somewhat distinct underlying properties of the transcriptional response to the stressor. These results also indicate that OA can affect genes involved in similar biological processes in different ways. For example, OA altered the developmental trajectory of some DNA repair genes, while other DNA repair genes showed a change in variance or transcript abundance in response to OA. Despite these effects, this functional category was not flagged by differential expression analysis as showing differences in expression level in response to OA. Although not widely applied in studies of stress response, analyses of variance, effect size, and trajectory clustering can enrich understanding of stress response at the molecular level, going beyond the insights gained from the traditional examination of differential expression in response to a stressor.

OA impacts expression of echinoderm-specific biomineralization genes

Biomineralization is a critical process for numerous marine organisms that use skeletons for defense, feeding, motility, and other important functions. The trend seen in many marine calcifiers in response to OA is production of less biomineral, resulting in smaller body size (Byrne & Fitzer, 2019; Kroeker et al., 2013). Skeletons likely evolved independently in several metazoan phyla, given their distinct biochemical, developmental, and genetic bases. This is almost certainly true of echinoderms (Bottjer, Davidson, Peterson, & Cameron, 2006; Shashikant, Khor, & Ettensohn, 2018a; A. M. Smith et al., 2016). Phylum-specific traits create a challenge when

interpreting transcriptomic results, because gene ontologies are based on annotations produced in model organisms that lack the biological process or trait of interest.

Fortunately, echinoderm-specific biomineralization gene sets have been compiled based on a wealth of molecular, biochemical, and developmental information (Ameye et al., 2001; Karakostis et al., 2016; Killian & Wilt, 2008, 2017; Shashikant et al., 2018a). Two independently derived gene sets are available (see Methods) and both showed enrichments in gene expression responses to OA in *H. erythrogramma*. These encompassed embryo and larva, but not metamorphosing juvenile (Table 2). The absence of enrichment of biomineralization in metamorphosing juveniles is surprising, given that this stage appears more vulnerable to the effects of OA (pHNIST 7.7) than earlier stages based on survivorship and skeletal morphology (Byrne et al., 2011; Wolfe, Dworjanyn, & Byrne, 2013) and shows by far the largest number of differentially expressed genes (Fig. 3A). The observation that both embryos and larvae show an OA-sensitive enrichment in biomineralization genes is expected, as the developmental processes that produce the larval skeleton begin in the early embryo (Shashikant, Khor, & Ettensohn, 2018b). Several prior studies identified individual genes involved in biomineralization that are OA-responsive in sea urchins (Di Giglio et al., 2020; Martin et al., 2011; O'Donnell et al., 2010; Stumpp et al., 2011) but we are not aware of any prior study in echinoderms that found an enriched transcriptional response to OA among biomineralization genes as a functional class using an unbiased approach.

Interestingly, while the details of the response in gene expression differ between studies, the overall results point to biomineralization as a clear indicator of OA stress in *H. erythrogramma,* as is generally the case for the life stages of sea urchins and other calcifiers, as expressed in responses from molecular to morphological levels (Byrne & Fitzer, 2019; Byrne et al., 2013; Kroeker et al., 2013; Maas et al., 2018; Strader et al., 2020).

586 ***Molecular responses to OA change substantially across the life cycle***

587 An important finding of this study is the substantial degree to which the molecular response
588 to OA changes across the life cycle. These differences among developmental stages were manifest
589 in every facet of the molecular response examined here: (1) transcript abundance changed markedly
590 in both overall magnitude and sign among stages (Figure 2), as did the identity of the genes
591 themselves (Figure 7); (2) the VMR changed for the transcriptome as a whole during development,
592 as did the specific transcripts whose VMR increased at low pH; 3) the portion of expression
593 variance attributable to pH across samples was elevated in dozens of genes; and (4) many
594 transcripts showed an altered developmental trajectory independent of abundance. While there was
595 some overlap among the specific transcripts that responded to OA between stages, most were
596 flagged as OA-responsive at only one stage (Fig. 3A; Fig. 8); this was true of all three criteria
597 examined (differential abundance, variance, trajectory). The three bulk metrics of OA response
598 reported here (average VMR, magnitude, and sign of response) also changed appreciably between
599 stages, indicating broad impacts on the transcriptome that differ across the life cycle (Fig. 8). Taken
600 together, these results indicate that examining any one developmental stage provides a strictly
601 limited view of the response to OA and that results from a single stage cannot be assumed to apply
602 to other phases of the life cycle.

603 This is not an unexpected result. Developmental and physiological processes change
604 substantially across the life cycle, and this is clearly reflected in developmental transcriptomes of
605 sea urchins under normal conditions (Israel et al., 2016; Tu, Cameron, & Davidson, 2014; Wong,
606 Gaitan-Espitia, & Hofmann, 2019; Wygoda et al., 2014). Importantly, these changing
607 developmental processes may render some life history stages particularly susceptible to stressors
608 (Hammond & Hofmann, 2012). This matters for OA because it is a chronic rather than an acute

stressor; examining one developmental stage may therefore miss important vulnerabilities. Indeed, prior work demonstrates that developmental stages of *H. erythrogramma* differ in sensitivity to OA (Byrne et al., 2009; Byrne et al., 2011; Hardy & Byrne, 2014). The distinct molecular responses to pH stress at different developmental stages identified in this study provide an important first step toward understanding why some stages of the life cycle are more vulnerable to OA than others.

Metamorphosis is particularly interesting as it is an exceptionally complex life stage in marine invertebrates, involving intricate coordination of developmental processes, extensive anatomical reorganization, and a major ecological transition from plankton to benthos. This life stage is particularly sensitive to stressors and is considered to be a mortality bottleneck for benthic species (Gosselin & Qian, 1997). Indeed, while early development of *H. erythrogramma* is resilient to OA, survivorship declines during the larva to juvenile metamorphic transition (Byrne et al., 2011; Wolfe et al., 2013), and spine development in the juveniles can be impaired at low pH (Wolfe et al., 2013). Here we observed both a larger number of differentially expressed genes and a marked bias towards down-regulation at pH_T 7.6 in metamorphosing juveniles (but not at earlier stages), which may indicate especially adverse effects of OA on metamorphosis. Due to the way we sampled (see Methods), individuals that developed through the larval stage to the early juvenile likely represent a subset of stress tolerant survivors with potentially biased loss of siblings according to genotype. Interestingly, however, juveniles also demonstrated deviations from average gene expression that were *less* stratified by pH at low pH than at control pH. It is possible that, while surviving juveniles are more susceptible to OA conditions than earlier stages, they represent a more genetically homogeneous cohort due to the cumulative effect of OA stress over developmental time, as well as the mortality bottleneck across the larva-to-juvenile metamorphic transition.

-

Stress-induced decanalization can confound measurements of transcriptional responses

The standard approach used to identify differential expression in RNA-seq data sets takes into account variance among biological samples (Anders et al., 2013; Conesa et al., 2016; Love et al., 2015; Zhang et al., 2014). While entirely appropriate in many situations, it is important to recognize that in a study of stress response, this approach can directly confound an informative biological response variable (i.e., loss of regulation) with the assessment of statistical significance. Stressors can cause dysregulation or loss of canalization, which can be reflected in increased variance in transcript abundance (Felix & Barkoulas, 2015; Lopez-Maury et al., 2008). To the extent that a stressor increases variance in gene expression, the standard approach to identifying differential expression introduces an ascertainment bias because it penalizes increased variance when determining whether a gene is differentially expressed. This artifact is likely absent from most transcriptomic analyses because the VMR does not change appreciably among samples (e.g., comparing successive developmental stages under normal conditions), but it is a clear concern when measuring a stress response that may be decanalizing.

Many genes with an elevated VMR at pH_T 7.6 in our results were not identified as differentially expressed by DESeq2 (despite showing a large change in mean), because variance increased substantially. Genes with a substantially elevated VMR at low pH included *Unc44_175* (SPU_025667), which encodes an ankyrin (proteins that connect integral membrane proteins to the cytoskeleton); *Ndufa13* (SPU_024115), which encodes an oxidoreductase (specifically, part of a protein complex that regulates cell death); and *Sushi* (SPU_002010) and *Egfi3* (SPU_011308), both of which encode fibropellins (proteins that regulate cell proliferation) (Fig. 5). These genes are all involved in regulatory processes, and two of the proteins bind calcium ions, making them interesting candidates for functional analysis. These examples illustrate how applying variance-

based metrics can identify candidate genes that would be missed by standard tests for differential expression when studying stress response.

Molecular responses to OA are modest relative to developmental changes

A noteworthy feature of the transcriptomic response of *H. erythrogramma* development to OA is its modest scale and scope. While thousands of genes rapidly change expression during normal development in sea urchins (Israel et al., 2016; Tu et al., 2014; Wong et al., 2019; Wygoda et al., 2014), fewer than 100 changed in response to OA in embryos and larvae, and fewer than 1,000 were altered in metamorphosing juveniles. Furthermore, the magnitude of expression changes under conditions of reduced pH was modest, with only a small fraction exceeding 1.5-fold (Fig. 2). In comparison, expression changes > 100-fold are common during development (Israel et al., 2016; Tu et al., 2014; Wong et al., 2019; Wygoda et al., 2014).

The expression of *Msp130* (SPU_002088) provides an instructive example. This gene encodes glycoprotein that plays a key role in transport of Ca^{2+} ions from the cell surface to the growing biomineral matrix (Anstrom et al., 1987; Karakostis et al., 2016; Killian & Wilt, 2017; Leaf et al., 1987; Mann, Poustka, & Mann, 2008). *Msp130* expression increased 1.82-fold and 1.54-fold at pH_T 7.6 in *H. erythrogramma* embryos and larvae, respectively. Prior studies have reported changes in *Msp130* expression of a comparable magnitude under OA conditions (Di Giglio et al., 2020; Kurihara et al., 2012; Martin et al., 2011; Stumpp et al., 2011). However, these stress responses are small compared to changes in *Msp130* expression levels during normal development (Israel et al., 2016; Tu et al., 2014; Wong et al., 2019; Wygoda et al., 2014). In *H. erythrogramma*, *Msp130* expression increased ~30-fold between embryo and larva and ~1000-fold between embryo and juvenile under control conditions (Supp. Fig. 2; note log2 scale). These large changes in

677 *Msp130* transcription during normal development suggest that caution is warranted when
678 considering the biological implications of the much smaller expression responses to OA.

679 ***Molecular responses to OA are eclipsed by the impact of natural genetic variation***

680 Two independent analytical approaches, principal components analysis and linear mixed
681 models, both indicated that natural genetic variation had a much larger overall impact on gene
682 expression than pH stress. In the linear mixed model, developmental stage explained on average
683 48.9% of expression variation per gene, male parent 6.5%, and pH just 0.2% (Supp. Data 3). Since
684 male genotype can be considered a proxy for genetic effects (Lynch & Walsh, 1998), our results
685 suggest that natural populations of *H. erythrogramma* contain extensive genetic variation that alters
686 gene expression to a greater degree than does exposure to OA. This finding is consistent with
687 studies of development of sea urchins with planktotrophic larvae (Pespeni et al., 2013; Runcie et
688 al., 2016) and similar findings for a coral (Jury, Delano, & Toonen, 2019) and a bivalve (Bitter,
689 Kapsenberg, Gattuso, & Pfister, 2019). Collectively, these studies suggest that it is not uncommon
690 for standing genetic variation to contribute more to interindividual phenotypic variation in gene
691 expression across the transcriptome than does OA.

692 Genetic variation that influences gene expression during development could, in principle,
693 provide genotypes that facilitate adaptation to OA in natural populations (Glazier et al., 2020;
694 Goncalves et al., 2016; Pespeni et al., 2013; Runcie et al., 2016). A previous study found that
695 development and settlement success of *H. erythrogramma* under OA conditions were both strongly
696 influenced by male parent (Foo, Dworjanyn, Poore, Harianto, & Byrne, 2016). Further, the ability
697 of individual male *H. erythrogramma* sperm to fertilize eggs differs between OA and control
698 conditions (K. E. Smith et al., 2019), suggesting genotype-by-phenotype interactions based in
699 segregating variation. If health and survivorship under OA conditions are mediated in part by

changes in gene expression, resilience to OA may differ among individuals in a population based in part on genetic variation. However, it should be noted that the interaction term (pH:Sire) in the linear mixed model also explained only a very small amount of variation in gene expression (0.3%). Furthermore, our experiment was not designed to detect such effects, as evidenced by the lack of replication within each cross. Further experiments will therefore be necessary to determine whether there exists sufficient genetic variation to provide the raw materials for natural selection to overcome the impacts of OA.

ACKNOWLEDGEMENTS

We thank the Sydney Institute of Marine Science (SIMS) for facilities, as well as the SIMS staff for their assistance. We also thank the staff of Duke's Sequencing and Genomic Technologies Shared Resource for help with RNA-seq. Members of the Byrne and Wray lab groups provided valuable input and advice throughout. This study was supported by a Graduate Research Fellowship from the NSF to HD, IOS1457305 and IOS1929934 from the NSF to GW, and DP150102771 from the ARC to MB. This is SIMS contribution number XXXX.

-

REFERENCES

[dataset] Devens, H., Davidson, P., Deaker, D., Smith, K.E., Wray, G., & Byrne, M.; 2020. Data accompanying "Ocean acidification induces distinct transcriptomic responses across life history stages of the sea urchin *Heliocidaris erythrogramma*." Dryad Digital Repository; doi:10.5061/dryad.3xsj3txdm

Albright, R., Caldeira, L., Hosfelt, J., Kwiatkowski, L., Maclaren, J. K., Mason, B. M., . . . Caldeira, K. (2016). Reversal of ocean acidification enhances net coral reef calcification. *Nature, 531*(7594), 362-365. doi:10.1038/nature17155

Altschul, S. F., Gish, W., Miller, W., Myers, E. W., & Lipman, D. J. (1990). Basic local alignment search tool. *J Mol Biol, 215*(3), 403-410. doi:10.1016/S0022-2836(05)80360-2

Ameye, L., De Becker, G., Killian, C., Wilt, F., Kemps, R., Kuypers, S., & Dubois, P. (2001). Proteins and saccharides of the sea urchin organic matrix of mineralization: characterization and localization in the spine skeleton. *J Struct Biol, 134*(1), 56-66. doi:10.1006/jsbi.2001.4361

Anders, S., McCarthy, D. J., Chen, Y. S., Okoniewski, M., Smyth, G. K., Huber, W., & Robinson, M. D. (2013). Count-based differential expression analysis of RNA sequencing data using R and Bioconductor. *Nature Protocols, 8*(9), 1765-1786. doi:10.1038/nprot.2013.099

Andrews, S. (2010). FastQC: a quality control tool for high throughput sequence data.

Anstrom, J. A., Chin, J. E., Leaf, D. S., Parks, A. L., & Raff, R. A. (1987). Localization and expression of msp130, a primary mesenchyme lineage-specific cell surface protein in the sea urchin embryo. *Development, 101*(2), 255-265.

Benjamini, Y., Drai, D., Elmer, G., Kafkafi, N., & Golani, I. (2001). Controlling the false discovery rate in behavior genetics research. *Behav Brain Res, 125*(1-2), 279-284.

Bitter, M. C., Kapsenberg, L., Gattuso, J. P., & Pfister, C. A. (2019). Standing genetic variation fuels rapid adaptation to ocean acidification. *Nat Commun, 10*(1), 5821. doi:10.1038/s41467-019-13767-1

Bolger, A. M., Lohse, M., & Usadel, B. (2014). Trimmomatic: a flexible trimmer for Illumina sequence data. *Bioinformatics, 30*(15), 2114-2120. doi:10.1093/bioinformatics/btu170

Bottjer, D. J., Davidson, E. H., Peterson, K. J., & Cameron, R. A. (2006). Paleogenomics of echinoderms. *Science, 314*(5801), 956-960. doi:10.1126/science.1132310

Byrne, M., & Fitzer, S. (2019). The impact of environmental acidification on the microstructure and mechanical integrity of marine invertebrate skeletons. *Conserv Physiol, 7*(1), coz062. doi:10.1093/conphys/coz062

Byrne, M., & Hernandez, J. C. (2020). Sea urchins in a high CO2 world: impacts of climate warming and ocean acidification across life history stages. In J. M. Laurence (Ed.), *Sea Urchines: Biology and Ecology* (Fourth ed., pp. 281-297): Elsevier B.V.

Byrne, M., Ho, M., Selvakumaraswamy, P., Nguyen, H. D., Dworjanyn, S. A., & Davis, A. R. (2009). Temperature, but not pH, compromises sea urchin fertilization and early development under near-future climate change scenarios. *Proc Biol Sci, 276*(1663), 1883-1888. doi:10.1098/rspb.2008.1935

Byrne, M., Ho, M., Wong, E., Soars, N. A., Selvakumaraswamy, P., Shepard-Brennand, H., . . . Davis, A. R. (2011). Unshelled abalone and corrupted urchins: development of marine calcifiers in a changing ocean. *Proc Biol Sci, 278*(1716), 2376-2383. doi:10.1098/rspb.2010.2404

Byrne, M., Lamare, M., Winter, D., Dworjanyn, S. A., & Uthicke, S. (2013). The stunting effect of a high CO2 ocean on calcification and development in sea urchin larvae, a synthesis from

the tropics to the poles. *Philos Trans R Soc Lond B Biol Sci, 368*(1627), 20120439. doi:10.1098/rstb.2012.0439

Byrne, M., & Sewell, M. A. (2019). Evolution of maternal lipid provisioning strategies in echinoids with non-feeding larvae: selection for high-quality juveniles. *Marine Ecology Progress Series, 616*, 95-106. doi:10.3354/meps12938

Byrne, M., Soars, N. A., Ho, M. A., Wong, E., McElroy, D., Selvakumaraswamy, P., . . . Davis, A. R. (2010). Fertilization in a suite of coastal marine invertebrates from SE Australia is robust to near-future ocean warming and acidification. *Marine Biology, 157*(9), 2061-2069. doi:10.1007/s00227-010-1474-9

Carey, N., Harianto, J., & Byrne, M. (2016). Sea urchins in a high-CO2 world: partitioned effects of body size, ocean warming and acidification on metabolic rate. *Journal of Experimental Biology, 219*(8), 1178-1186. doi:10.1242/jeb.136101

Chen, J., Nolte, V., & Schlotterer, C. (2015). Temperature stress mediates decanalization and dominance of gene expression in Drosophila melanogaster. *PLoS Genet, 11*(2), e1004883. doi:10.1371/journal.pgen.1004883

Collard, M., Catarino, A. I., Bonnet, S., Flammang, P., & Dubois, P. (2013). Effects of CO2-induced ocean acidification on physiological and mechanical properties of the starfish Asterias rubens. *Journal of Experimental Marine Biology and Ecology, 446*, 355-362. doi:10.1016/j.jembe.2013.06.003

Conesa, A., Madrigal, P., Tarazona, S., Gomez-Cabrero, D., Cervera, A., McPherson, A., . . . Mortazavi, A. (2016). A survey of best practices for RNA-seq data analysis. *Genome Biol, 17*, 13. doi:10.1186/s13059-016-0881-8

Dalman, M. R., Deeter, A., Nimishakavi, G., & Duan, Z. H. (2012). Fold change and p-value cutoffs significantly alter microarray interpretations. *Bmc Bioinformatics, 13 Suppl 2*, S11. doi:10.1186/1471-2105-13-S2-S11

Davidson, P. L., Thompson, J. W., Foster, M. W., Moseley, M. A., Byrne, M., & Wray, G. A. (2019). A comparative analysis of egg provisioning using mass spectrometry during rapid life history evolution in sea urchins. *Evolution & Development, 21*(4), 188-204. doi:10.1111/ede.12289

Davies, S. W., Marchetti, A., Ries, J. B., & Castillo, K. D. (2016). Thermal and pCO(2) Stress Elicit Divergent Transcriptomic Responses in a Resilient Coral. *Frontiers in Marine Science, 3*. doi:10.3389/fmars.2016.00112

De Wit, P., Durland, E., Ventura, A., & Langdon, C. J. (2018). Gene expression correlated with delay in shell formation in larval Pacific oysters (Crassostrea gigas) exposed to experimental ocean acidification provides insights into shell formation mechanisms. *Bmc Genomics, 19*(1), 160. doi:10.1186/s12864-018-4519-y

Di Giglio, S., Spatafora, D., Milazzo, M., M'Zoudi, S., Zito, F., Dubois, P., & Costa, C. (2020). Are control of extracellular acid-base balance and regulation of skeleton genes linked to resistance to ocean acidification in adult sea urchins? *Science of The Total Environment*, 137443. doi:https://doi.org/10.1016/j.scitotenv.2020.137443

Dickson, A. G. (1990). Standard potential of the reaction: AgCl(s) + 12H2(g) = Ag(s) + HCl(aq), and and the standard acidity constant of the ion HSO4− in synthetic sea water from 273.15 to 318.15 K. *The Journal of Chemical Thermodynamics, 22*(2), 113-127. doi:https://doi.org/10.1016/0021-9614(90)90074-Z

Dickson, A. G., & Millero, F. J. (1987). A comparison of the equilibrium constants for the dissociation of carbonic acid in seawater media. *Deep Sea Research Part A. Oceanographic Research Papers, 34*(10), 1733-1743. doi:https://doi.org/10.1016/0198-0149(87)90021-5

Dickson, A. G., Sabine, C.L., & Christian, J.R. (2007). Guide to best practices for ocean CO2 measurements. . *PICES Special Publication, 3*, 191.

Dunn, C. W., Howison, M., & Zapata, F. (2013). Agalma: an automated phylogenomics workflow. *BMC Bioinformatics, 14*, 330. doi:10.1186/1471-2105-14-330

Emlet, R. B. (1995). Larval spicules, cilia, and symmetry as remnants of indirect development in the direct developing sea urchin Heliocidaris erythrogramma. *Developmental Biology, 167*(2), 405-415. doi:10.1006/dbio.1995.1037

Evans, T. G., Chan, F., Menge, B. A., & Hofmann, G. E. (2013). Transcriptomic responses to ocean acidification in larval sea urchins from a naturally variable pH environment. *Molecular Ecology, 22*(6), 1609-1625. doi:10.1111/mec.12188

Evans, T. G., Pespeni, M. H., Hofmann, G. E., Palumbi, S. R., & Sanford, E. (2017). Transcriptomic responses to seawater acidification among sea urchin populations inhabiting a natural pH mosaic. *Molecular Ecology, 26*(8), 2257-2275. doi:10.1111/mec.14038

Evans, T. G., & Watson-Wynn, P. (2014). Effects of seawater acidification on gene expression: resolving broader-scale trends in sea urchins. *Biol Bull, 226*(3), 237-254. doi:10.1086/BBLv226n3p237

Felix, M. A., & Barkoulas, M. (2015). Pervasive robustness in biological systems. *Nature Reviews Genetics, 16*(8), 483-496. doi:10.1038/nrg3949

Foo, S. A., Dworjanyn, S. A., Poore, A. G. B., Harianto, J., & Byrne, M. (2016). Adaptive capacity of the sea urchin Heliocidaris erythrogramma to ocean change stressors: responses from gamete performance to the juvenile. *Marine Ecology Progress Series, 556*, 161-172.

Gattuso, J. P., Magnan, A., Bille, R., Cheung, W. W. L., Howes, E. L., Joos, F., . . . Turley, C. (2015). Contrasting futures for ocean and society from different anthropogenic CO2 emissions scenarios. *Science, 349*(6243). doi:10.1126/science.aac4722

Glazier, A., Herrera, S., Weinnig, A., Kurman, M., Gomez, C. E., & Cordes, E. (2020). Regulation of ion transport and energy metabolism enables certain coral genotypes to maintain calcification under experimental ocean acidification. *Molecular Ecology*. doi:10.1111/mec.15439

Goncalves, P., Anderson, K., Thompson, E. L., Melwani, A., Parker, L. m., Ross, P. M., & Raftos, D. A. (2016). Rapid transcriptional acclimation following transgenerational exposure of oysters to ocean acidification. *Molecular Ecology, 25*(19), 4836-4849. doi:10.1111/mec.13808

Gosselin, L. A., & Qian, P.-Y. (1997). Juvenile mortality in benthic marine invertebrates. *Marine Ecology Progress Series, 146*(1/3), 265-282.

Grabherr, M. G., Haas, B. J., Yassour, M., Levin, J. Z., Thompson, D. A., Amit, I., . . . Regev, A. (2011). Full-length transcriptome assembly from RNA-Seq data without a reference genome. *Nat Biotechnol, 29*(7), 644-652. doi:10.1038/nbt.1883

Griffiths, J. S., Pan, T.-C. F., & Kelly, M. W. (2019). Differential responses to ocean acidification between populations of Balanophyllia elegans corals from high and low upwelling environments. *Molecular Ecology, 28*(11), 2715-2730. doi:10.1111/mec.15050

Hammond, L. M., & Hofmann, G. E. (2012). Early developmental gene regulation in Strongylocentrotus purpuratus embryos in response to elevated CO(2) seawater conditions. *J Exp Biol, 215*(Pt 14), 2445-2454. doi:10.1242/jeb.058008

Hardy, N. A., & Byrne, M. (2014). Early development of congeneric sea urchins (Heliocidaris) with contrasting life history modes in a warming and high CO2 ocean. *Mar Environ Res, 102*, 78-87. doi:10.1016/j.marenvres.2014.07.007

Henry, J. J., & Raff, R. A. (1990). Evolutionary change in the process of dorsoventral axis determination in the direct developing sea urchin, Heliocidaris erythrogramma. *Developmental Biology, 141*(1), 55-69.

Henry, J. J., Wray, G. A., & Raff, R. A. (1990). The dorsoventral axis is specified prior to first cleavage in the direct developing sea urchin Heliocidaris erythrogramma. *Development, 110*(3), 875-884.

Hoffman, G. E., & Schadt, E. E. (2016). variancePartition: interpreting drivers of variation in complex gene expression studies. *Bmc Bioinformatics, 17*(1), 483. doi:10.1186/s12859-016-1323-z

IPCC. (2014). Climate change 2014: synthesis report. Contribution of Working Groups I, II and III to the fifth assessment report of the Intergovernmental Panel on Climate Change. *Geneva, Switzerland: IPCC*.

Israel, J. W., Martik, M. L., Byrne, M., Raff, E. C., Raff, R. A., McClay, D. R., & Wray, G. A. (2016). Comparative Developmental Transcriptomics Reveals Rewiring of a Highly Conserved Gene Regulatory Network during a Major Life History Switch in the Sea Urchin Genus Heliocidaris. *PLoS Biol, 14*(3), e1002391. doi:10.1371/journal.pbio.1002391

Jury, C. P., Delano, M. N., & Toonen, R. J. (2019). High heritability of coral calcification rates and evolutionary potential under ocean acidification. *Sci Rep, 9*(1), 20419. doi:10.1038/s41598-019-56313-1

Karakostis, K., Zanella-Cleon, I., Immel, F., Guichard, N., Dru, P., Lepage, T., . . . Marin, F. (2016). A minimal molecular toolkit for mineral deposition? Biochemistry and proteomics of the test matrix of adult specimens of the sea urchin Paracentrotus lividus. *J Proteomics, 136*, 133-144. doi:10.1016/j.jprot.2016.01.001

Keesing, J. K. (2020). Heliocidaris erythrogramma. In J. M. Lawrence (Ed.), Sea Urchins: Biology and Ecology (Fourth
ed., pp. 537-552): Elsevier B.V.

Killian, C. E., & Wilt, F. H. (2008). Molecular aspects of biomineralization of the echinoderm endoskeleton. *Chem Rev, 108*(11), 4463-4474. doi:10.1021/cr0782630

Killian, C. E., & Wilt, F. H. (2017). Endocytosis in primary mesenchyme cells during sea urchin larval skeletogenesis. *Exp Cell Res, 359*(1), 205-214. doi:10.1016/j.yexcr.2017.07.028

Kroeker, K. J., Kordas, R. L., Crim, R., Hendriks, I. E., Ramajo, L., Singh, G. S., . . . Gattuso, J. P. (2013). Impacts of ocean acidification on marine organisms: quantifying sensitivities and interaction with warming. *Glob Chang Biol, 19*(6), 1884-1896. doi:10.1111/gcb.12179

Kumar, L., & Futschik, E. (2007). Mfuzz: a software package for soft clustering of microarray data. *Bioinformation, 2*(1), 5-7.

Kurihara, H., Takano, Y., Kurokawa, D., & Akasaka, K. (2012). Ocean acidification reduces biomineralization-related gene expression in the sea urchin, Hemicentrotus pulcherrimus. *Marine Biology, 159*(12), 2819-2826. doi:10.1007/s00227-012-2043-1

Langmead, B., & Salzberg, S. L. (2012). Fast gapped-read alignment with Bowtie 2. *Nature Methods, 9*(4), 357-U354. doi:10.1038/Nmeth.1923

Leaf, D. S., Anstrom, J. A., Chin, J. E., Harkey, M. A., Showman, R. M., & Raff, R. A. (1987). Antibodies to a fusion protein identify a cDNA clone encoding msp130, a primary mesenchyme-specific cell surface protein of the sea urchin embryo. *Developmental Biology, 121*(1), 29-40. doi:10.1016/0012-1606(87)90135-7

Li, W., & Godzik, A. (2006). Cd-hit: a fast program for clustering and comparing large sets of protein or nucleotide sequences. *Bioinformatics, 22*(13), 1658-1659. doi:10.1093/bioinformatics/btl158

Liu, Z., Zhang, Y., Zhou, Z., Zong, Y., Zheng, Y., Liu, C., . . . Song, L. (2020). Metabolomic and transcriptomic profiling reveals the alteration of energy metabolism in oyster larvae during initial shell formation and under experimental ocean acidification. *Sci Rep, 10*(1), 6111. doi:10.1038/s41598-020-62963-3

Lopez-Maury, L., Marguerat, S., & Bahler, J. (2008). Tuning gene expression to changing environments: from rapid responses to evolutionary adaptation. *Nature Reviews Genetics, 9*(8), 583-593. doi:10.1038/nrg2398

Love, M. I., Anders, S., Kim, V., & Huber, W. (2015). RNA-Seq workflow: gene-level exploratory analysis and differential expression. *F1000Res, 4*, 1070. doi:10.12688/f1000research.7035.1

Love, M. I., Huber, W., & Anders, S. (2014). Moderated estimation of fold change and dispersion for RNA-seq data with DESeq2. *Genome Biol, 15*(12), 550. doi:10.1186/s13059-014-0550-8

Lynch, M., & Walsh, B. (1998). *Genetics and analysis of quantitative traits* (Vol. 1): Sinauer Sunderland, MA.

Maas, A. E., Lawson, G. L., Bergan, A. J., & Tarrant, A. M. (2018). Exposure to CO2 influences metabolism, calcification and gene expression of the thecosome pteropod Limacina retroversa. *J Exp Biol, 221*(Pt 3). doi:10.1242/jeb.164400

Mann, K., Poustka, A. J., & Mann, M. (2008). The sea urchin (Strongylocentrotus purpuratus) test and spine proteomes. *Proteome Sci, 6*, 22. doi:10.1186/1477-5956-6-22

Mark, S., Weiss, J., Sharma, E., Liu, T., Wang, W., Claycomb, J. M., & Cutter, A. D. (2019). Genome structure predicts modular transcriptome responses to genetic and environmental conditions. *Molecular Ecology, 28*(16), 3681-3697. doi:10.1111/mec.15185

Martin, S., Richier, S., Pedrotti, M. L., Dupont, S., Castejon, C., Gerakis, Y., . . . Gattuso, J. P. (2011). Early development and molecular plasticity in the Mediterranean sea urchin Paracentrotus lividus exposed to CO2-driven acidification. *J Exp Biol, 214*(Pt 8), 1357-1368. doi:10.1242/jeb.051169

Mehrbach, C., Culberson, C. H., Hawley, J. E., & Pytkowicx, R. M. (1973). MEASUREMENT OF THE APPARENT DISSOCIATION CONSTANTS OF CARBONIC ACID IN SEAWATER AT ATMOSPHERIC PRESSURE1. *Limnology and Oceanography, 18*(6), 897-907. doi:10.4319/lo.1973.18.6.0897

Micallef, L., & Rodgers, P. (2014). eulerAPE: Drawing Area-Proportional 3-Venn Diagrams Using Ellipses. *Plos One, 9*(7). doi:ARTN e101717

10.1371/journal.pone.0101717

O'Donnell, M. J., Todgham, A. E., Sewell, M. A., Hammond, L. M., Ruggiero, K., Fangue, N. A., . . . Hofmann, G. E. (2010). Ocean acidification alters skeletogenesis and gene expression in larval sea urchins. *Marine Ecology Progress Series, 398*, 157-171. doi:10.3354/meps08346

Padilla-Gamino, J. L., Kelly, M. W., Evans, T. G., & Hofmann, G. E. (2013). Temperature and CO2 additively regulate physiology, morphology and genomic responses of larval sea urchins, Strongylocentrotus purpuratus. *Proceedings of the Royal Society B-Biological Sciences, 280*(1759). doi:ARTN 20130155

10.1098/rspb.2013.0155

Pan, T. C., Applebaum, S. L., & Manahan, D. T. (2015). Experimental ocean acidification alters the allocation of metabolic energy. *Proc Natl Acad Sci U S A, 112*(15), 4696-4701. doi:10.1073/pnas.1416967112

Patro, R., Duggal, G., Love, M. I., Irizarry, R. A., & Kingsford, C. (2017). Salmon provides fast and bias-aware quantification of transcript expression. *Nat Methods, 14*(4), 417-419. doi:10.1038/nmeth.4197

Pespeni, M. H., Sanford, E., Gaylord, B., Hill, T. M., Hosfelt, J. D., Jaris, H. K., . . . Palumbi, S. R. (2013). Evolutionary change during experimental ocean acidification. *Proc Natl Acad Sci U S A, 110*(17), 6937-6942. doi:10.1073/pnas.1220673110

Pierrot, D., E. Lewis, and D. Wallace. (2006). MS Excel program developed for CO2 system calculations, ORNL/CDIAC-105a. U.S. Dep. of Energy, Oak Ridge, Tenn.: Oak Ridge Natl. Lab.

Przeslawski, R., Byrne, M., & Mellin, C. (2015). A review and meta-analysis of the effects of multiple abiotic stressors on marine embryos and larvae. *Glob Chang Biol, 21*(6), 2122-2140. doi:10.1111/gcb.12833

Rafiq, K., Shashikant, T., McManus, C. J., & Ettensohn, C. A. (2014). Genome-wide analysis of the skeletogenic gene regulatory network of sea urchins. *Development, 141*(4), 950-961. doi:10.1242/dev.105585

Runcie, D. E., Dorey, N., Garfield, D. A., Stumpp, M., Dupont, S., & Wray, G. A. (2016). Genomic Characterization of the Evolutionary Potential of the Sea Urchin Strongylocentrotus droebachiensis Facing Ocean Acidification. *Genome Biology and Evolution, 8*(12), 3672-3684. doi:10.1093/gbe/evw272

Ryan, J. F. (2015). Alien Index (Version 1.0): Zenodo.

Schurch, N. J., Schofield, P., Gierlinski, M., Cole, C., Sherstnev, A., Singh, V., . . . Barton, G. J. (2016). How many biological replicates are needed in an RNA-seq experiment and which differential expression tool should you use? *RNA, 22*(6), 839-851. doi:10.1261/rna.053959.115

Sea Urchin Genome Sequencing, C., Sodergren, E., Weinstock, G. M., Davidson, E. H., Cameron, R. A., Gibbs, R. A., . . . Wright, R. (2006). The genome of the sea urchin Strongylocentrotus purpuratus. *Science, 314*(5801), 941-952. doi:10.1126/science.1133609

Shashikant, T., Khor, J. M., & Ettensohn, C. A. (2018a). From genome to anatomy: The architecture and evolution of the skeletogenic gene regulatory network of sea urchins and other echinoderms. *Genesis, 56*(10), e23253. doi:10.1002/dvg.23253

Shashikant, T., Khor, J. M., & Ettensohn, C. A. (2018b). Global analysis of primary mesenchyme cell cis-regulatory modules by chromatin accessibility profiling. *Bmc Genomics, 19*(1), 206. doi:10.1186/s12864-018-4542-z

Smith, A. M., Clark, D. E., Lamare, M. D., Winter, D. J., & Byrne, M. (2016). Risk and resilience: variations in magnesium in echinoid skeletal calcite. *Marine Ecology Progress Series, 561*, 1-16. doi:10.3354/meps11908

Smith, K. E., Byrne, M., Deaker, D., Hird, C. M., Nielson, C., Wilson-McNeal, A., & Lewis, C. (2019). Sea urchin reproductive performance in a changing ocean: poor males improve while good males worsen in response to ocean acidification. *Proceedings of the Royal Society B-Biological Sciences, 286*(1907). doi:10.1098/rspb.2019.0785

Smith, M. S., Collins, S., & Raff, R. A. (2009). Morphogenetic mechanisms of coelom formation in the direct-developing sea urchin Heliocidaris erythrogramma. *Development Genes and Evolution, 219*(1), 21-29. doi:10.1007/s00427-008-0262-8

Smith-Unna, R., Boursnell, C., Patro, R., Hibberd, J. M., & Kelly, S. (2016). TransRate: reference-free quality assessment of de novo transcriptome assemblies. *Genome Res, 26*(8), 1134-1144. doi:10.1101/gr.196469.115

Soneson, C., Love, M. I., & Robinson, M. D. (2015). Differential analyses for RNA-seq: transcript-level estimates improve gene-level inferences. *F1000Res, 4*, 1521. doi:10.12688/f1000research.7563.2

Strader, M. E., Wong, J. M., & Hofmann, G. E. (2020). Ocean acidification promotes broad transcriptomic responses in marine metazoans: a literature survey. *Front Zool, 17*, 7. doi:10.1186/s12983-020-0350-9

Stumpp, M., Wren, J., Melzner, F., Thorndyke, M. C., & Dupont, S. T. (2011). CO2 induced seawater acidification impacts sea urchin larval development I: elevated metabolic rates

decrease scope for growth and induce developmental delay. *Comp Biochem Physiol A Mol Integr Physiol, 160*(3), 331-340. doi:10.1016/j.cbpa.2011.06.022

Todgham, A. E., & Hofmann, G. E. (2009). Transcriptomic response of sea urchin larvae Strongylocentrotus purpuratus to CO2-driven seawater acidification. *J Exp Biol, 212*(Pt 16), 2579-2594. doi:10.1242/jeb.032540

Tu, Q., Cameron, R. A., & Davidson, E. H. (2014). Quantitative developmental transcriptomes of the sea urchin Strongylocentrotus purpuratus. *Developmental Biology, 385*(2), 160-167. doi:10.1016/j.ydbio.2013.11.019

Uppström, L. R. (1974). *The boron/chlorinity ratio of deep-sea water from the Pacific Ocean*. https://ui.adsabs.harvard.edu/abs/1974DSROA..21..161U

Uthicke, S., Schaffelke, B., & Byrne, M. (2009). A boom–bust phylum? Ecological and evolutionary consequences of density variations in echinoderms. *Ecological Monographs, 79*(1), 3-24. doi:10.1890/07-2136.1

Varemo, L., Nielsen, J., & Nookaew, I. (2013). Enriching the gene set analysis of genome-wide data by incorporating directionality of gene expression and combining statistical hypotheses and methods. *Nucleic Acids Research, 41*(8), 4378-4391. doi:10.1093/nar/gkt111

Walker, N. S., Fernández, R., Sneed, J. M., Paul, V. J., Giribet, G., & Combosch, D. J. (2019). Differential gene expression during substrate probing in larvae of the Caribbean coral Porites astreoides. *Molecular Ecology, 28*(22), 4899-4913. doi:10.1111/mec.15265

Webster, A. K., Jordan, J. M., Hibshman, J. D., Chitrakar, R., & Baugh, L. R. (2018). Transgenerational Effects of Extended Dauer Diapause on Starvation Survival and Gene Expression Plasticity in Caenorhabditis elegans. *Genetics, 210*(1), 263-274. doi:10.1534/genetics.118.301250

Williams, D., & Anderson, D. (1975). The reproductive system, embryonic development, larval development and metamorphosis of the sea urchin Heliocidaris erythrogramma (Val.) (Echinoidea : Echinometridae). *Australian Journal of Zoology, 23*(3), 371-403. doi:https://doi.org/10.1071/ZO9750371

Wolfe, K., Dworjanyn, S. A., & Byrne, M. (2013). Effects of ocean warming and acidification on survival, growth and skeletal development in the early benthic juvenile sea urchin (Heliocidaris erythrogramma). *Global Change Biology, 19*(9), 2698-2707. doi:10.1111/gcb.12249

Wolfe, K., Nguyen, H. D., Davey, M., & Byrne, M. (2020). Characterizing biogeochemical fluctuations in a world of extremes: A synthesis for temperate intertidal habitats in the face of global change. *Glob Chang Biol, 26*(7), 3858-3879. doi:10.1111/gcb.15103

Wong, J. M., Gaitan-Espitia, J. D., & Hofmann, G. E. (2019). Transcriptional profiles of early stage red sea urchins (Mesocentrotus franciscanus) reveal differential regulation of gene expression across development. *Mar Genomics, 48*, 100692. doi:10.1016/j.margen.2019.05.007

Wong, J. M., Johnson, K. M., Kelly, M. W., & Hofmann, G. E. (2018). Transcriptomics reveal transgenerational effects in purple sea urchin embryos: Adult acclimation to upwelling conditions alters the response of their progeny to differential pCO2 levels. *Molecular Ecology, 27*(5), 1120-1137. doi:10.1111/mec.14503

Wray, G. A., & Raff, R. A. (1990). Novel origins of lineage founder cells in the direct-developing sea urchin Heliocidaris erythrogramma. *Developmental Biology, 141*(1), 41-54.

Wygoda, J. A., Yang, Y., Byrne, M., & Wray, G. A. (2014). Transcriptomic Analysis of the Highly Derived Radial Body Plan of a Sea Urchin. *Genome Biology and Evolution, 6*(4), 964-973. doi:10.1093/gbe/evu070

-

Zhang, Z. H., Jhaveri, D. J., Marshall, V. M., Bauer, D. C., Edson, J., Narayanan, R. K., . . . Zhao, Q. Y. (2014). A comparative study of techniques for differential expression analysis on RNA-Seq data. *Plos One, 9*(8), e103207. doi:10.1371/journal.pone.0103207

-

TABLE LEGENDS

Table 1. Previous gene expression studies on various sea urchin species in response to experimental ocean acidification.

Table 2. Enrichment of Gene Ontology (GO) and echinoderm-specific gene sets and pathways (see *Methods*) in the set of differentially-expressed genes between the two pH levels used in this study. PMC effector genes (Rafiq, Shashikant, McManus, & Ettensohn, 2014) are marked with an asterisk.

-

FIGURE LEGENDS

Figure 1. Experimental design (left) and analytical pipeline of RNA-seq data (right).

Figure 2. Stage-by-stage differential gene expression at A) embryo, B) larvae, and C) juvenile. Pink represents differentially expressed genes supported by an adjusted p-value < 10% and log2(FC) < 1.5. Red represents differentially expressed genes supported by an adjusted p-value <10% and log2(FC) >= 1.5. Grey represents genes that were not differentially expressed. Positive FC values are genes more highly expressed at pH_T 8.0; negative FC values are genes more highly expressed at pH_T 7.6.

Figure 3. Overlap between stage- and criterion-specific sets of transcriptional responses to OA. Exact area-proportional Euler diagrams (scaled Venn diagrams) are shown representing the total number of genes identified and their overlaps. A) Differentially expressed (DE) genes at three life history stages. B) Gene expression responses to reduced pH_T according to three distinct criteria: change in transcript abundance (DE), increased proportion of variance explained by pH_T (variance) and altered developmental trajectory (cluster jump). See text for an explanation of inclusion criteria.

Figure 4. A) Principal component analysis of transcript abundances across all samples. B) Variance partitioning of gene expression attributed to each factor of the experimental design. PC: principal component.

Figure 5. Average variance-to-mean (VMR) ratio for pH_T 8.0 (blue) and 7.6 (red) at A) embryo, B) larva, and C) juvenile. VMR is significantly higher at for embryo and larval stages (two-sided paired t-test; *: p-value < 5e-2; **: p-value < 5e-7). Mean vs variance plots at D) embryo, E) larva, and F) juvenile showing that difference in VMR between pH_T conditions at the larval stage is attributable to lower variance (y-axis) at pH_T 8.0, not changes in mean expression (x-axis). G-

H) Examples of genes with higher expression variance among replicates at pH_T 7.6 relative to pH_T 8.0, highlighted in panels D-F. G) *sushi*; H) *ankyrin2,3*; I) NADH−ubiquinone oxidoreductase B16.6 subunit; J) fibropellin 1. Blue: pH_T 8.0. Red: pH_T 7.6.

Figure 6. Comparative soft clustering analyses of 10,404 genes between pH_T 8.0 and 7.6. Time course plots on each axis describe five temporal expression patterns at pH_T 8.0 (blue) and pH_T 7.6 (red), respectively. Each grid entry represents the number of genes with a change (or lack thereof) in developmental expression pattern between pH_T 8.0 and 7.6. For example, 2270 genes (top left) had no change in developmental expression pattern at pH_T 8.0 and pH_T 7.6. In contrast, 2 genes (top right) that decreased in expression through development at pH_T 8.0 instead increased in expression at pH_T 7.6. Purple shading describes the proportion of genes with each expression trajectory change between pH_T conditions.

Figure 7. Density distribution of the deviation for each male parental genotype from the mean expression across all genotypes, for all genes. Deviation was calculated as relative change. K-S tests were performed for each combination of genotypes at each stage; the distribution of each genotype (in both pH conditions and at all stages) was found to be statistically different from that of all other genotypes within the stage and pH condition ($p<0.05$).

Figure 8. Subset of pH_T sensitive genes identified by three independent types of analyses carried out in this study: stage-by-stage differential expression, variance partitioning of factor contribution to expression, and comparative time course “cluster jumping” genes.

SUPPLEMENTARY TABLE LEGENDS

Supplementary Table 1. Carbonate chemistry parameters describing set up of flow-through sea water system in which *Heliocidaris erythrogramma* was reared. Data displayed as averages ± SE, n = 5.

Supplementary Table 2. Sequencing strategy and sample information of each RNA-seq sample collected. One sample, 8_1M1L, was not sequenced due to poor RNA quality.

Supplementary Table 3. Summary statistics of *de-novo* assembled transcriptome. "mean ORF %" denotes mean percentage of contig covered by an open reading frame (ORF), for those contigs with an ORF. Statistics generated with Transrate (Smith-Unna et al., 2016).

Supplementary Table 4. Summary of variance explained by principal components from PCA.

Supplementary Table 5. Differentially expressed genes in our study that were also found to be differentially expressed in other species and/or stages in other studies (See *Methods* for studies used). 890 OA-responsive genes from other studies were compared to 908 DE genes in this study; 131 genes were common to the two sets.

Supplementary Table 6. Genes that were differentially expressed at more than one stage. Sign indicates the direction of expression change at pH_T 7.6 relative to control pH_T 8.0.

-

SUPPLEMENTARY FIGURE LEGENDS

Supplementary Figure 1. Timecourse cluster profiles generated by the *Mfuzz* package (Kumar & Futschik, 2007) based on gene expression from all stages and pH conditions studied.

Supplementary Figure 2. Expression timecourse of *Msp130* in control (pH_T 8.0; blue) and OA (pH_T 7.6; red) conditions.

Supplementary Figure 3. Density plots of VMR (also known as "dispersion index") for pH_t 8.0 (blue) and 7.6 (red) at each developmental stage: A) embryo, B) larva, C) juvenile

Supplementary Figure 4. Density plots of VMR (also known as "dispersion index") for all genes, broken down by gene functional category according to Echinobase.

DATA ACCESSIBILITY

Sequencing reads and the transcriptome generated in this study are publicly available on Dryad Digital Repository (doi:10.5061/dryad.3xsj3txdm). Transcript abundances and gene sets are available in the Supplementary Data online.

AUTHOR CONTRIBUTIONS

M.B. conceived the study. D.J.D., K.E.S., and M.B. designed and set up the experiment. P.L.D., D.J.D., K.E.S., and M.B. performed the sample collection. H.R.D. and P.L.D. analyzed the data. H.R.D., P.L.D., G.A.W., and M.B. wrote the paper.

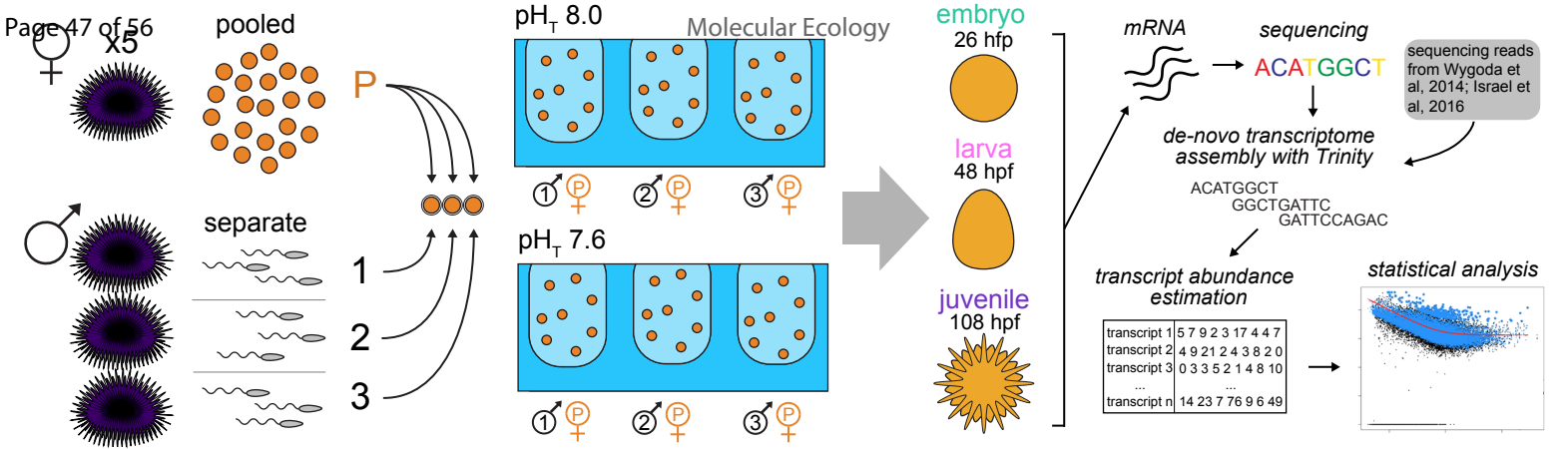
X5
pooled
P
separate
1
2
3
pH$_T$ 8.0
pH$_T$ 7.6
embryo
26 hfp
larva
48 hpf
juvenile
108 hpf
mRNA
sequencing
ACATGGCT
sequencing reads from Wygoda et al, 2014; Israel et al, 2016
de-novo transcriptome assembly with Trinity
ACATGGCT
GGCTGATTC
GATTCCAGAC
transcript abundance estimation
transcript 1 5 7 9 2 3 17 4 4 7
transcript 2 4 9 21 2 4 3 8 2 0
transcript 3 0 3 3 5 2 1 4 8 10
transcript n 14 23 7 76 9 6 49
statistical analysis

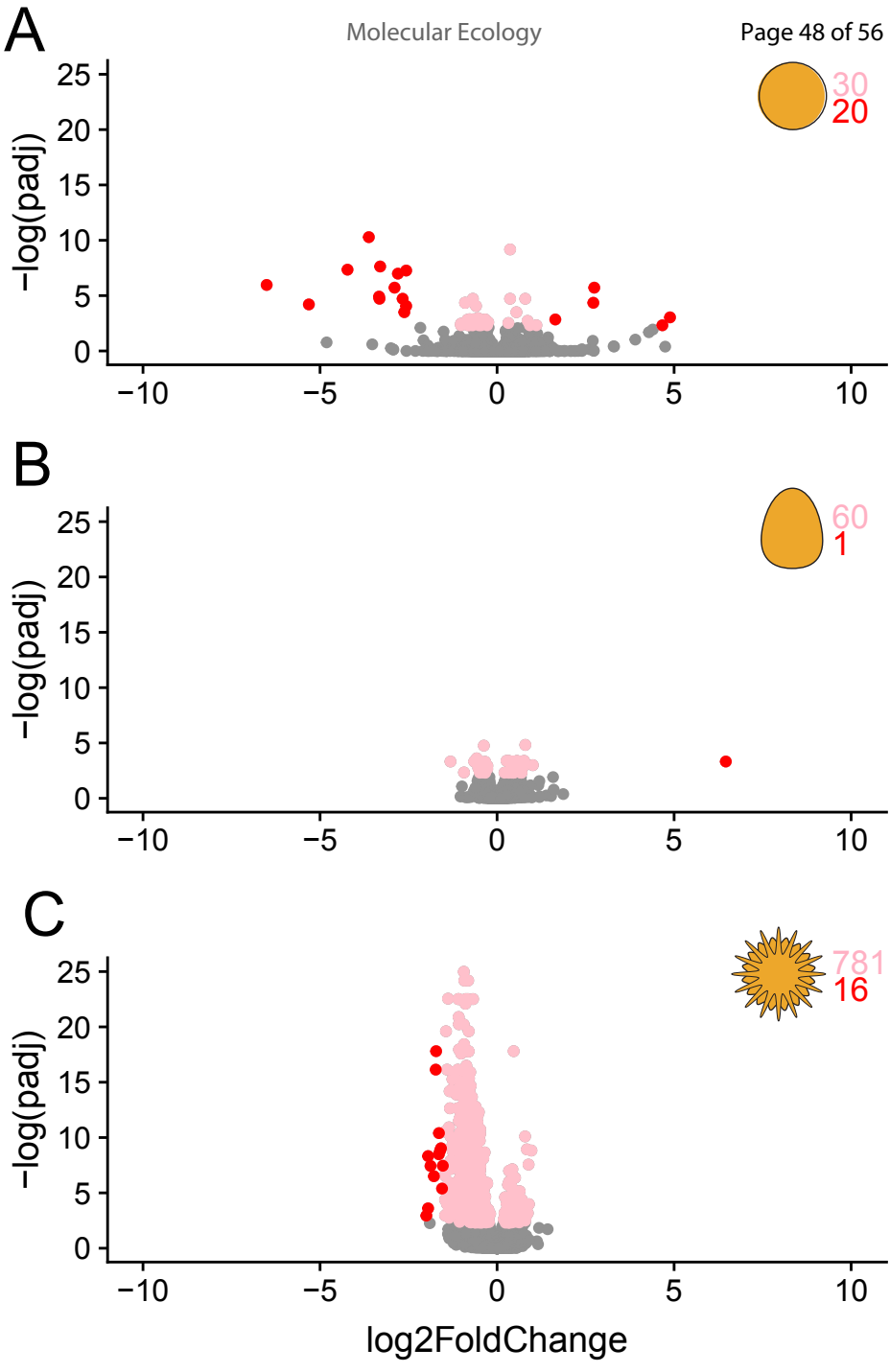
A
B
C
−log(padj)
log2FoldChange
30
20
60
1
781
16

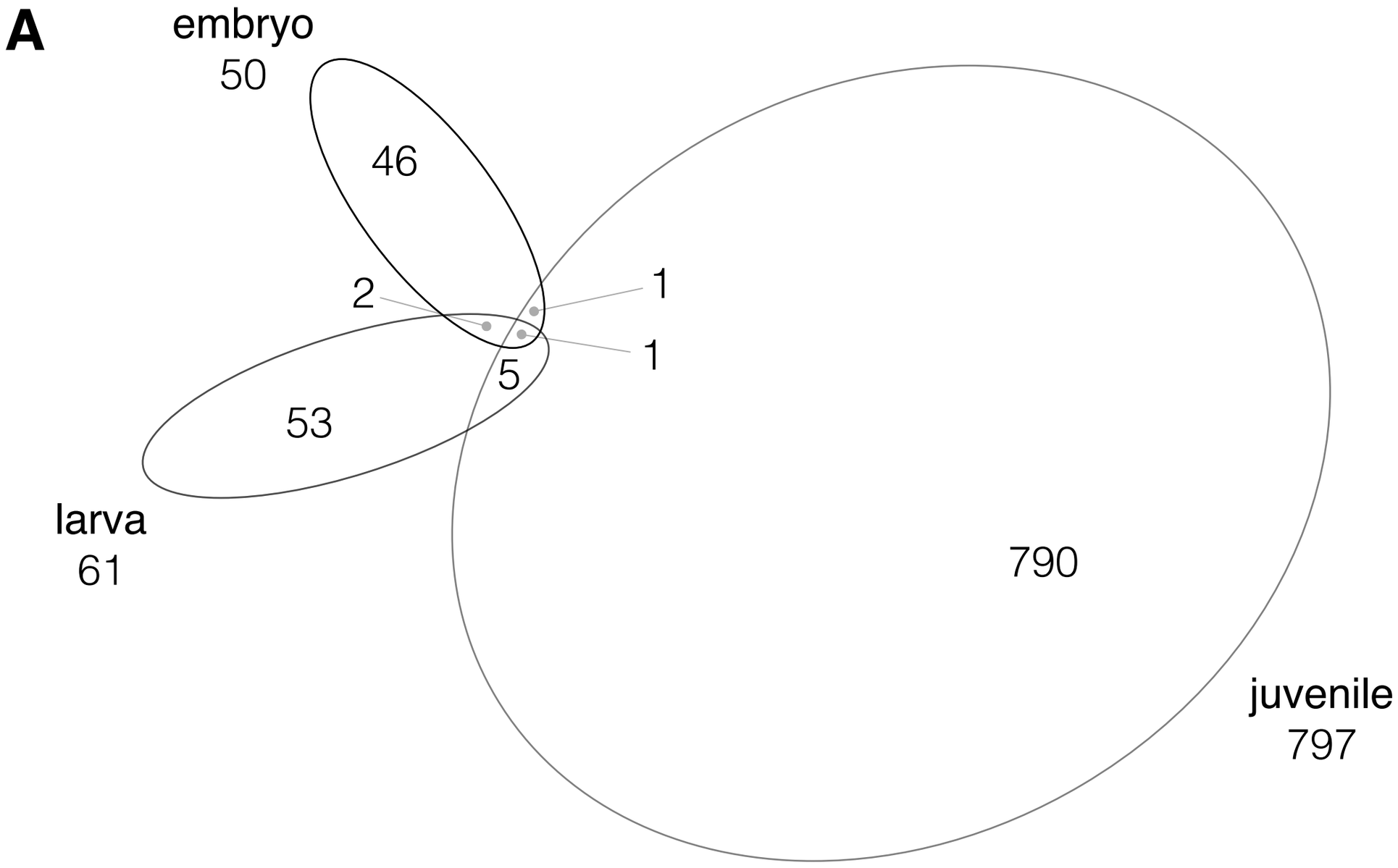
A
embryo
50
46
2
1
1
5
53
larva
61
790
juvenile
797

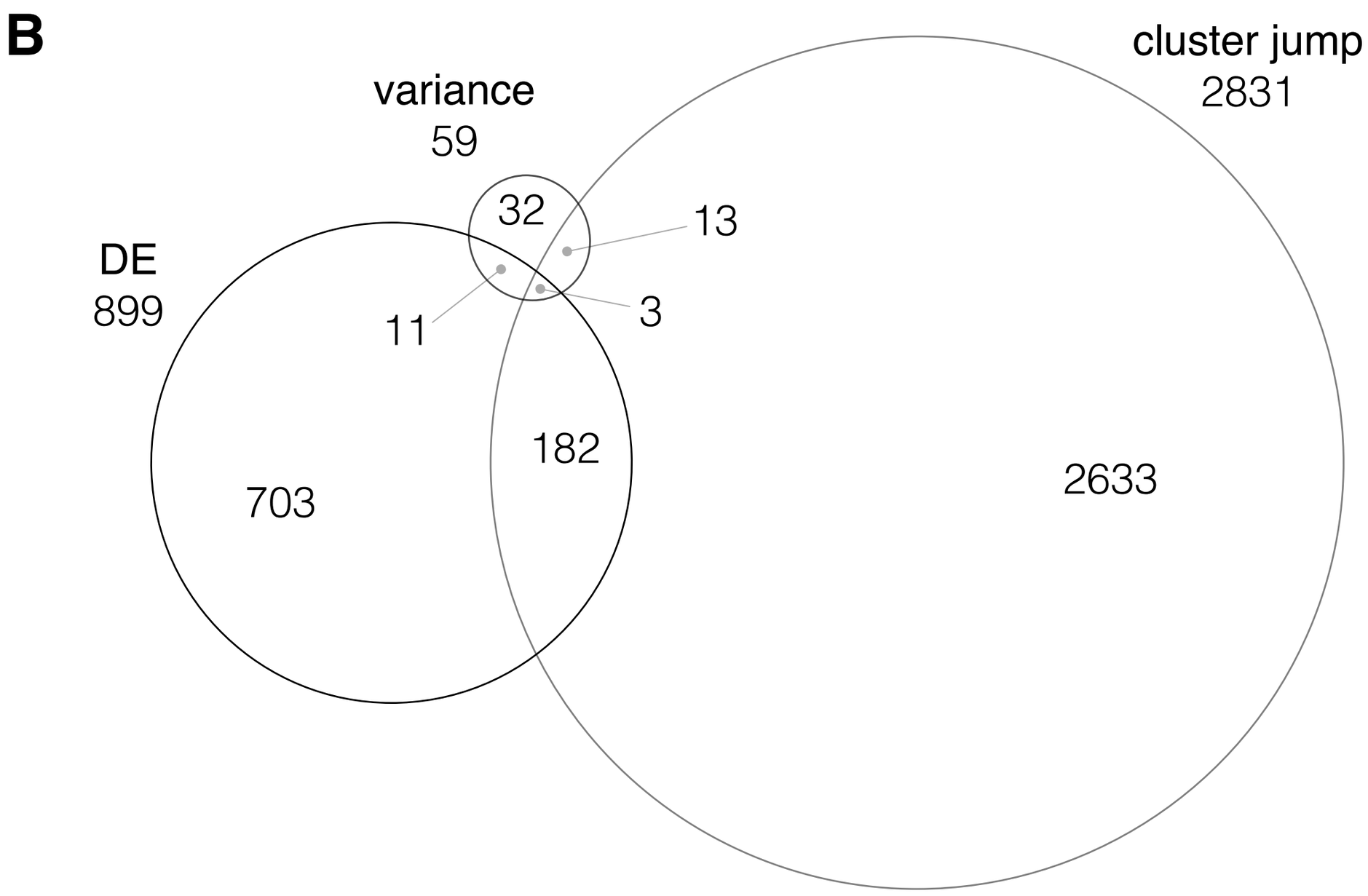
B
variance
59
cluster jump
2831
32
13
DE
899
11
3
182
703
2633

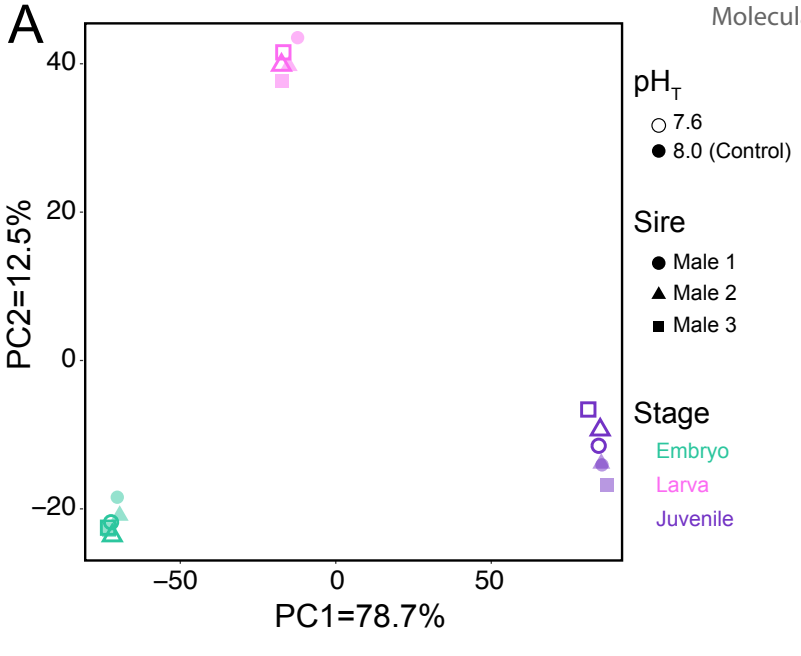
A
40
20
0
−20
PC2=12.5%
−50
0
50
PC1=78.7%
pH$_T$
7.6
8.0 (Control)
Sire
Male 1
Male 2
Male 3
Stage
Embryo
Larva
Juvenile

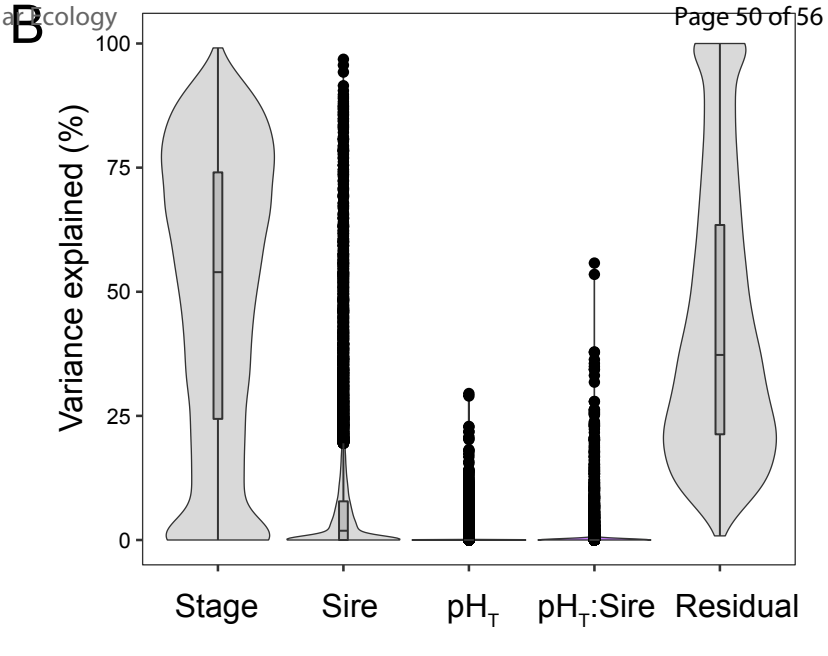
B
Variance explained (%)
100
75
50
25
0
Stage
Sire
pH$_T$
pH$_T$:Sire
Residual

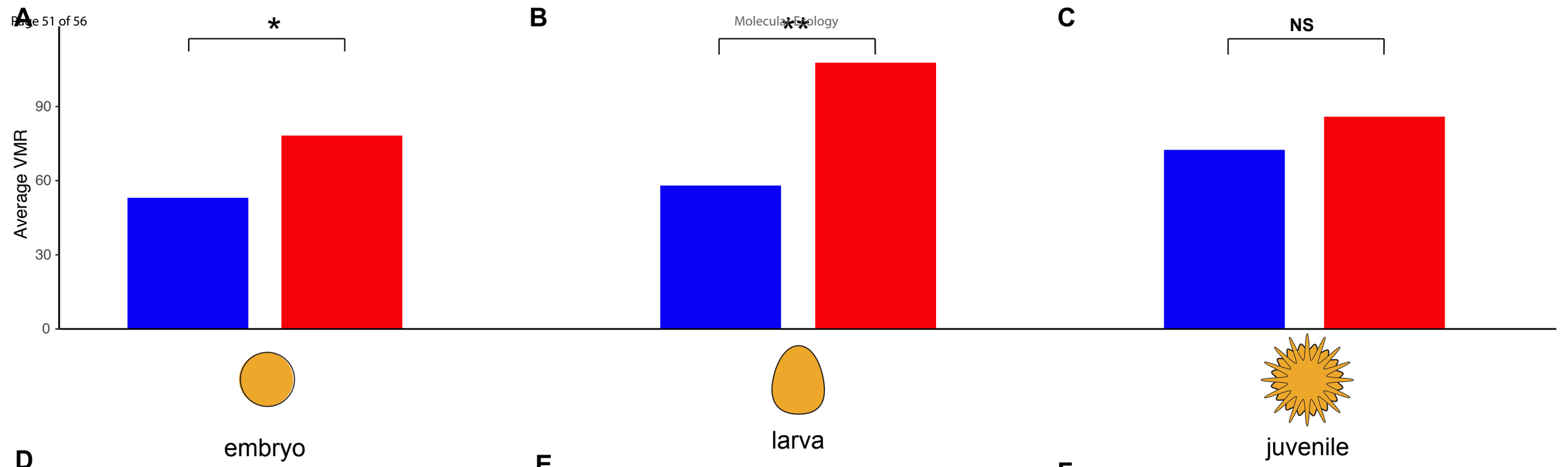
A
B
C
*
**
NS
Average VMR
0
30
60
90
embryo
larva
juvenile

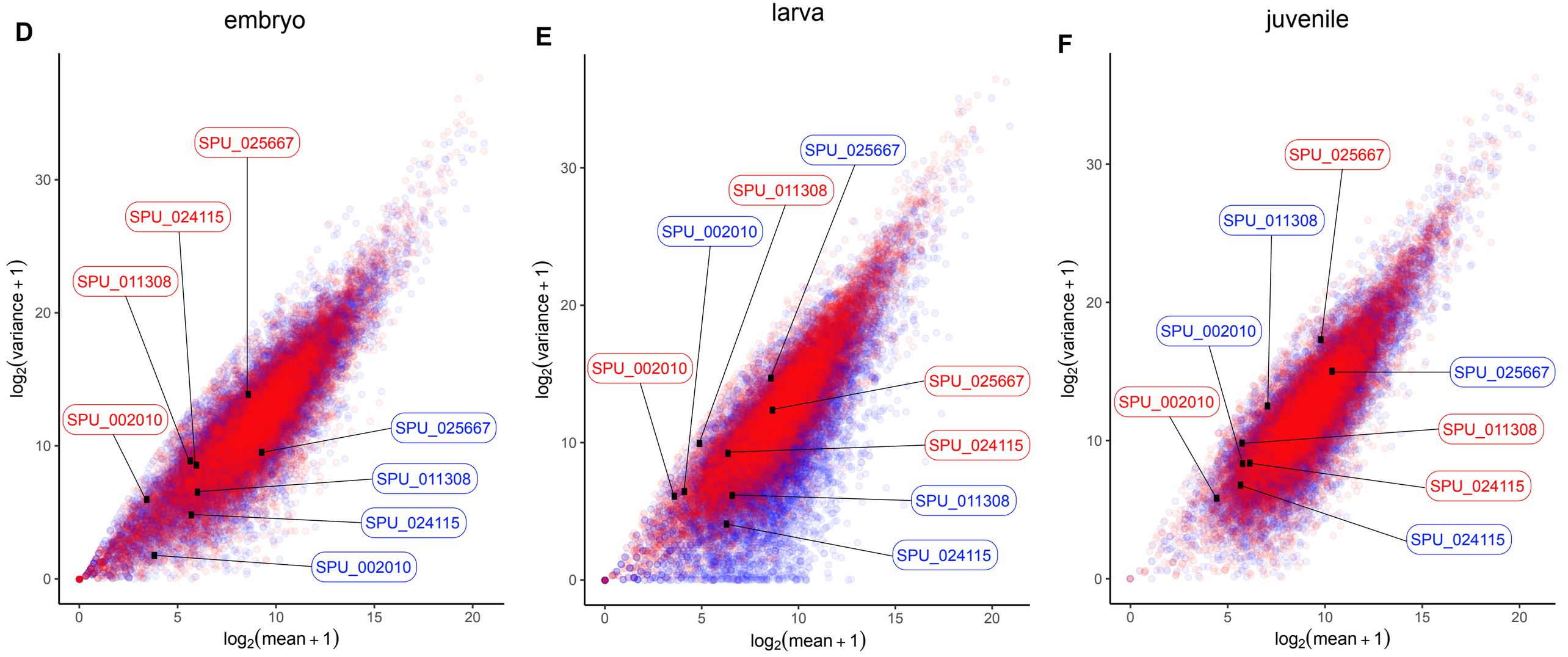
D
E
F
log2(variance + 1)
log2(mean + 1)
SPU_025667
SPU_024115
SPU_011308
SPU_002010

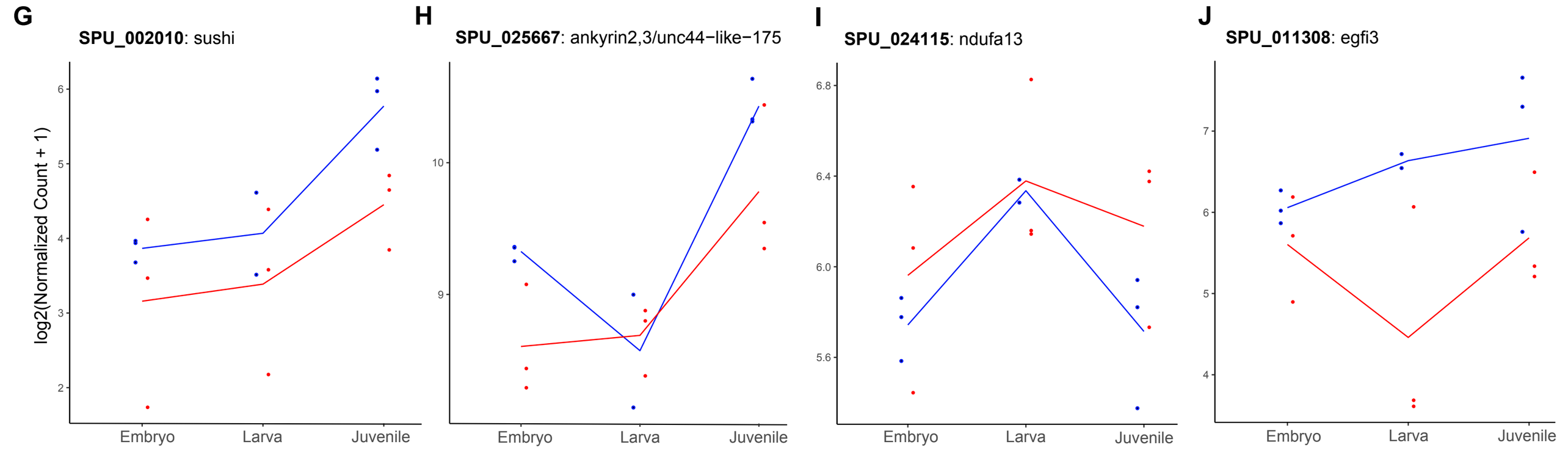
G
SPU_002010: sushi
H
SPU_025667: ankyrin2,3/unc44−like−175
I
SPU_024115: ndufa13
J
SPU_011308: egfi3
log2(Normalized Count + 1)
Embryo
Larva
Juvenile

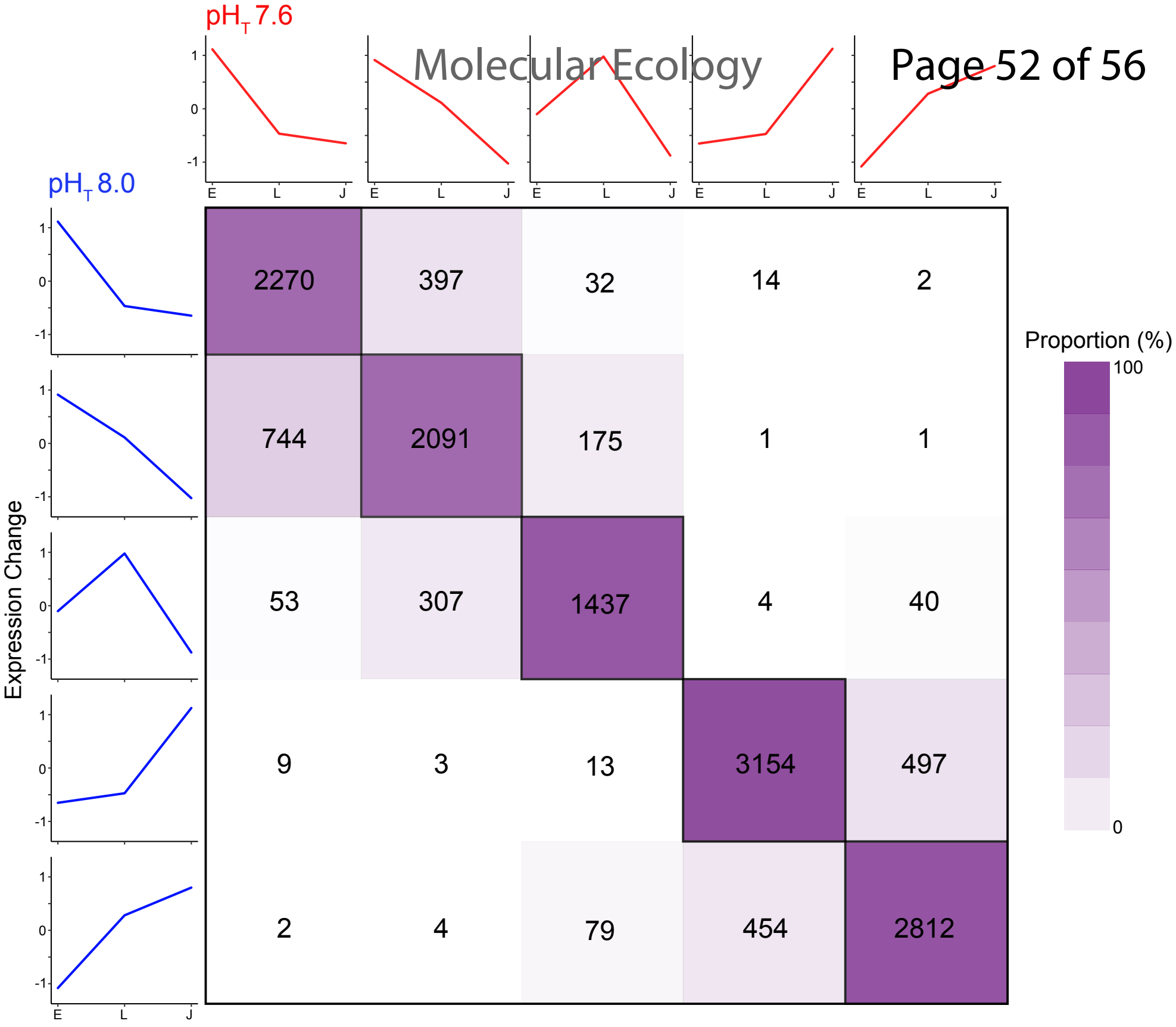
pH$_T$ 7.6
pH$_T$ 8.0
Expression Change
E
L
J
2270
397
32
14
2
744
2091
175
1
1
53
307
1437
4
40
9
3
13
3154
497
2
4
79
454
2812
Proportion (%)
100
0

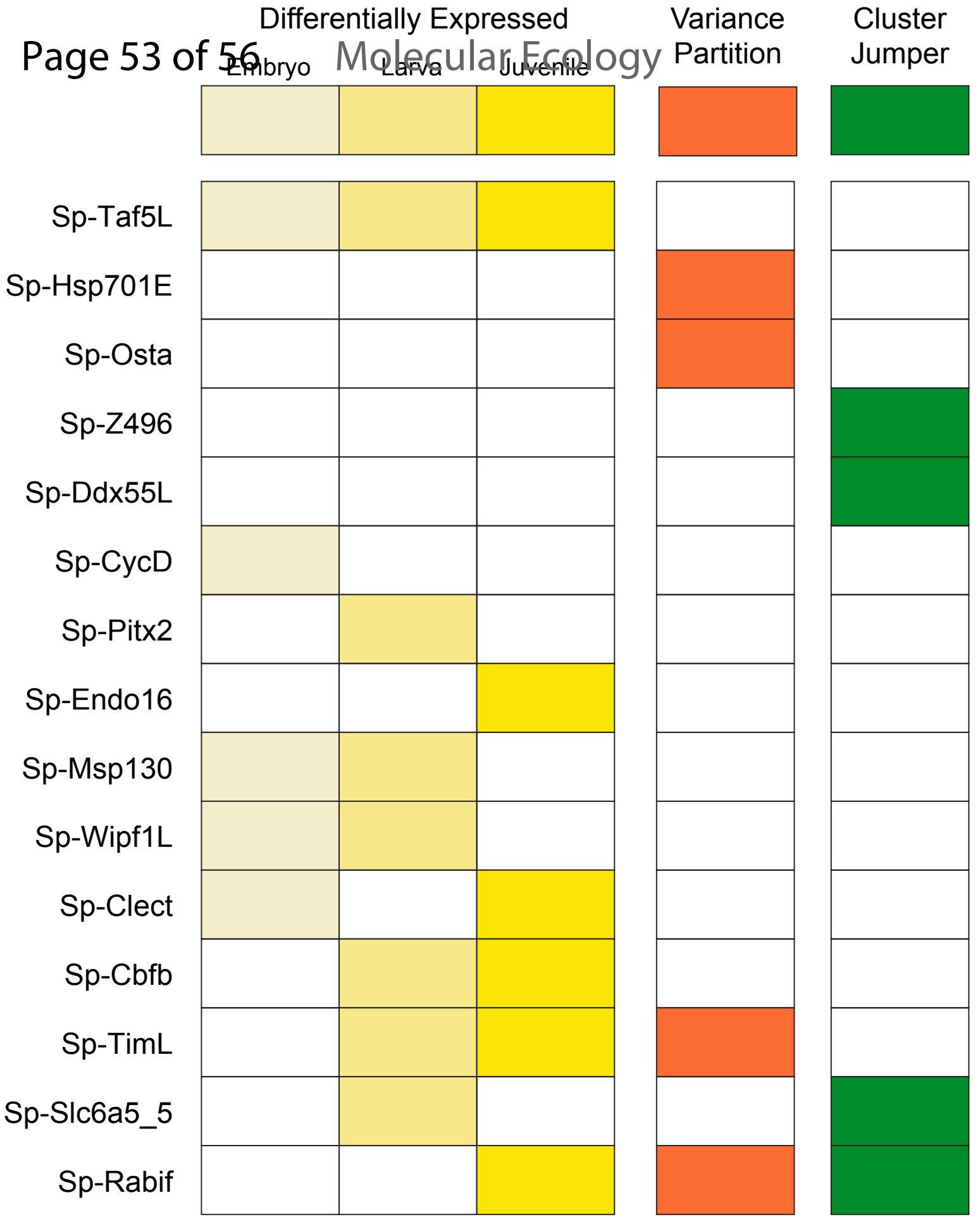
Differentially Expressed
Embryo
Larva
Juvenile
Variance Partition
Cluster Jumper
Sp-Taf5L
Sp-Hsp701E
Sp-Osta
Sp-Z496
Sp-Ddx55L
Sp-CycD
Sp-Pitx2
Sp-Endo16
Sp-Msp130
Sp-Wipf1L
Sp-Clect
Sp-Cbfb
Sp-TimL
Sp-Slc6a5_5
Sp-Rabif

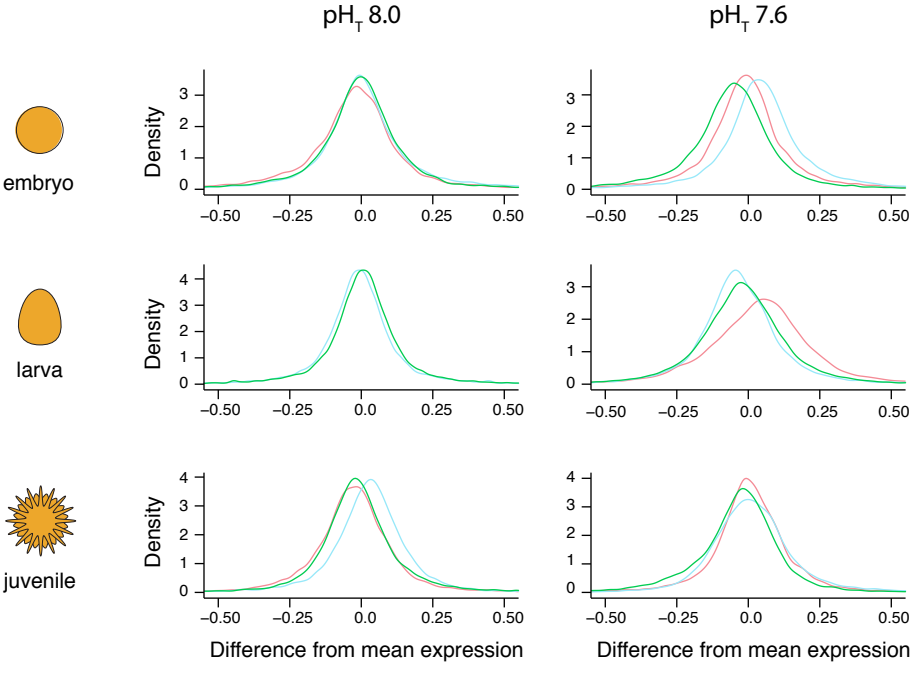
pH$_T$ 8.0
pH$_T$ 7.6
embryo
larva
juvenile
Density
Difference from mean expression
Sire
male 1
male 2
male 3

Species	Life History	Stage	Experimental pH used	Sequencing method	Reference
Hemicentrotus pulcherrimus	Planktotroph	Gastrula, Prism, Pluteus	7.75 7.45	rtPCR	Kurihara et al., 2012
Lytechinus pictus	Planktotroph	Pluteus	7.87 7.78	Microarray	O'Donnell et al., 2010
Paracentrotus lividus	Planktotroph	Gastrula, Pluteus	7.9 7.7 7.5 7.25 7.0	rtPCR	Martin et al., 2011
Strongylocentrotus deoebachiensis	Planktotroph	Pluteus	7.6	RNAseq	Runcie et al., 2016
Strongylocentrotus purpuratus	Planktotroph	Pluteus	7.7	Microarray	Stumpp et al., 2011
Strongylocentrotus purpuratus	Planktotroph	Adult (tube feet)	7.65-7.95 (field experiment)	RNAseq	Pespeni et al., 2013
Strongylocentrotus purpuratus	Planktotroph	Gastrula, Pluteus	400 μatm CO_2 900 μatm CO_2	RNAseq	Evans et al., 2017
Strongylocentrotus purpuratus	Planktotroph	Pluteus	7.77 7.59	Microarray	Evans et al., 2013
Strongylocentrotus purpuratus	Planktotroph	Gastrula	7.76 7.68	RNAseq	Wong, Johnson, Kelly, & Hofmann, 2018
Strongylocentrotus purpuratus	Planktotroph	Pluteus	7.96 7.88	Microarray	Todgham & Hofmann, 2009
Strongylocentrotus purpuratus	Planktotroph	Pluteus	1100 μatm pCO2	Microarray	Padilla-Gamino et al., 2013
Strongylocentrotus purpuratus	Planktotroph	Gastrula (3 stages)	7.69 7.62	rtPCR	Hammond & Hofmann, 2012

	Embryo	Larva	Juvenile
Genes	*SPU_007451	SPU_018406	SPU_010805
	*SPU_009476	SPU_002088	SPU_021344
	*SPU_008985	SPU_013821	SPU_000353
	*SPU_002148	SPU_013823	SPU_025378
	*SPU_016500		SPU_026146
	SPU_014496		SPU_013237
	SPU_002088		SPU_008175
	SPU_015763		
Categorical Enrichment	nucleotide catabolic process (<0.003)	nucleotide catabolic process (<0.006)	microtubule-based movement (<2.5e-6)
	regulation of transcription, DNA-templated (<0.006)	regulation of transcription, DNA-templated (<0.022)	microtubule cytoskeleton organization (<0.002)
	*PMC effector genes (<0.034)	biomineralization genes (<0.081)	cilium movement (<0.006)
	biomineralization genes (<0.034)		regulation of transcription, DNA-templated (<0.009)
			Wnt signaling pathway (<0.009)